NASA TECHNICAL NOTE

NASA TN D-5126

NASA TN D-5126

EXPLODING WIRE INITIATION AND ELECTRICAL OPERATION OF A 40-kV SYSTEM FOR ARC-HEATED DRIVERS UP TO 10 FEET LONG

by Robert E. Dannenberg and Anthony F. Silva

Ames Research Center
Moffett Field, Calif.

NATIONAL AERONAUTICS AND SPACE ADMINISTRATION • WASHINGTON, D. C. • APRIL 1969

NASA TN D-5126

EXPLODING WIRE INITIATION AND ELECTRICAL OPERATION OF A 40-kV SYSTEM FOR ARC-HEATED DRIVERS UP TO 10 FEET LONG

By Robert E. Dannenberg and Anthony F. Silva

Ames Research Center
Moffett Field, Calif.

NATIONAL AERONAUTICS AND SPACE ADMINISTRATION

For sale by the Clearinghouse for Federal Scientific and Technical Information
Springfield, Virginia 22151 – CFSTI price $3.00

EXPLODING WIRE INITIATION AND ELECTRICAL OPERATION OF A 40-kV SYSTEM FOR ARC-HEATED DRIVERS UP TO 10 FEET LONG

By Robert E. Dannenberg and Anthony F. Silva

Ames Research Center

SUMMARY

This report describes an energy storage and electric-arc driver system for shock-driven facilities. Energy for the arc is supplied from a capacitor bank rated at 1 MJ at an operating voltage of 40 kV. Results are presented for arc discharge lengths of 54 and 116 inches with peak currents of 600 kA. The entire arc strike sequence of exploding wire initiation, dwell period, and subsequent bank discharge is discussed. The effect of different wire types on arc initiation is also discussed. The composition of the driver gas is shown to be a factor that limits the discharge of stored energy from the capacitor bank.

INTRODUCTION

An electrically heated helium driver with an arc chamber up to 10 feet long has been developed for shock-driven facilities. The design of the arc driver is unique in that it can be used to power either of two parallel spaced facilities: A 30-inch shock tunnel for gasdynamic testing of models or a low-density shock tube for studies of nonequilibrium gas reactions. The shock tunnel requires a relatively long driver in order that adequate test times (~2 msec) can be realized in a tailored interface mode of operation (refs. 1 and 2). The useful test time is generally considered to end soon after the arrival at the nozzle throat section of the expansion wave that is reflected from the upstream end of the driver. The shock tube does not require a long driver; in fact, a shorter driver is advantageous. The primary requirement is for an energy density as high as possible (see refs. 3-6).

To achieve the desired tailored mode of operation in the shock tunnel, an energy density of about 45 J/cm^3 was estimated to be required to heat the driver gas. In addition, a long arc, about 10 feet long, was considered necessary to obtain a sufficient test time. Also, the high pressure arc demands a high driving potential. From these considerations, and for a driver diameter of 4 inches, the energy storage supply selected was rated at 1 MJ when charged to 40,000 V. For use in a low-density shock tube, the arc length of the driver would be reduced and the energy density increased accordingly. The length of the arc-heated driver, together with its energy storage system, is beyond the capabilities of most existing facilities, and, as such, is an interesting research tool in its own right.

This report presents data on the system performance, particularly in regard to the discharge phenomena, for arc lengths of 54 and 116 inches in a cylindrical driver. Current and voltage measurements were obtained over a wide range of voltages and gas loading pressures. Several different wire types were tried as arc initiators. Tests were made with different driver gas compositions.

GENERAL SYSTEM DESCRIPTION

The electric arc driver system was designed to provide a practical high-energy driver to be used with different types of shock-driven facilities. The driver is composed of two 5-foot, heavy-walled tube sections, one of which contains the current collector assembly. The latter section is designated as the 54-inch arc driver and when the two sections are connected, the arrangement is designated as the 116-inch arc driver. The system is quite versatile, and different driver combinations are available for use at two stations. In the arrangement shown in figure 1, the 54-inch driver is in position at a diaphragm test rig. A low-density shock tube is scheduled for installation at this station at a later date. For shock tube use, the arc chamber length can be reduced to at least 18 inches so that the energy density within the chamber will be high (~300 J/cm^3).

In the alternate position noted in figure 1, the driver powers a 30-inch hypersonic shock tunnel with a 4-inch I.D. driven tube that is 37 feet long. Both the 54- and 116-inch drivers have been tested at this station in the arrangements shown in figures 2 and 3, respectively. Pertinent details of the two driver sizes are given in table I, and a schematic assembly of the 116-inch driver is shown in figure 4. For a complete discharge of the stored energy from the capacitor bank into the arc chamber, the maximum obtainable energy density was 87 and 55 J/cm^3 for the 54- and 116-inch driver, respectively.

The energy for the arc is supplied by a 1250-μF capacitor bank that is capable of storing 1 million joules when charged to a maximum of 40,000 V. The bank is charged in about 90 seconds and the nominal discharge time is 325 μsec for a 10-foot arc strike. The arc is contained within the insulated arc chamber and is initiated by a fine tungsten trigger wire. The capacitor bank is connected and arranged for discharge at maximum voltage in fractions of maximum energy-storage capacity, or at a particular energy storage by varying the preset voltage. A detailed description of the energy storage and arc driver system is given in appendix A.

GENERAL ARC CHARACTERISTICS

The arc discharge phenomena associated with the electric arc driver will be discussed by considering the four distinct sequential modes in the cycle of operation: (1) a triggered gap switch, (2) the exploding wire, (3) a dwell period prior to the arc discharge, and (4) the arc discharge.

Triggered Gap Switch

When the driver is ready to fire, the space (occupied by the cotton thread) between the high-voltage electrode and the tip of the trigger wire acts as a gas gap or switch. It is the sole device preventing the capacitor bank energy from discharging. As the gap is reduced to a particular value, the breakdown voltage is reached and a slight ionization occurs, which causes a large pulse of electrical energy to pass through the wire in a short period of time.

Tests were made of the electrode-wire arrangement to determine the breakdown voltages for various gap widths in air and in helium. The results are shown in figure 5 and are generally referred to as "Paschen curves" (see ref. 7). The air data were obtained easily in a bench test with a hipot tester. The helium results were determined during operation of the driver by means of an FM transmitter mounted directly on the high-voltage current collector. In this arrangement, the FM telemetry afforded complete electrical isolation between the signal and receiver stations. The FM telemeter circuit, consisting of a simple Colpitts oscillator powered by two 1.3-V mercury cells, was similar to that described in reference 8. The oscillator was tuned by physically displacing the dielectric of the tuning capacitor. The dielectric, made of Teflon, was mechanically linked to the movement of the air cylinder (fig. 3). A change in the position of the trigger caused a corresponding change in the circuit tuning capacitance, resulting in a change in the telemeter carrier frequency. The carrier was received and detected by a standard broadband FM telemetry receiver at the ground station, whose output was calibrated to give trigger wire position. The gap spacing at arc discharge was determined as the onset of RFI noise induced by the arc itself (fig. 6).

Exploding Trigger Wire

With the gap breakdown, initial currents of the order of 10^4 A are developed and the trigger wire is exploded in times apparently less than 10^{-6} sec. The very fast, high-energy explosion leaves the metal of the wire in the probable form of a column of hot aerosol, with liquid beads dispersed in a gaseous mist. The RFI noise generated by the exploding wire also serves as the trigger source for the oscilloscope that records the discharge characteristics. A voltage and current waveform, typical of each arc length, is presented in figure 7. The current trace shown in figure 7(b) was recorded simultaneously with the telemetry record of figure 6. (Interesting X-ray and streak photographs of exploding wires are presented in refs. 9 and 10.)

Dwell Period

The exploding wire does not instantaneously induce the arc strike. In fact, the duration of the period from explosion to the start of the main discharge of energy from the capacitor bank was surprisingly long. This dwell period was about 100 to 150 μsec for a 54-inch arc and 400 to 500 μsec for a 116-inch arc (see figs. 7 and 8). The dwell period in the driver chamber is apparently one of low conductivity. Figure 8(b) shows a current trace for a

20:1 gain and an increased sweep speed. From this and similar records, it appears that the rate of current flow is low, probably not in excess of a few hundred amperes.

The mechanism that accounts for the long dwell period is not fully understood. In fact, the mechanism of the wire explosion (and arc discharge) is at best but partly explained. Some parts of the process are without explanation, and others have been explained by a number of theories. For the arc driver, the duration of the dwell interval is believed to be associated with the high initial inductance of the long trigger wire compared to the small inductance of the remainder of the system. For example, the system inductance is only 0.25 μH compared to 2.3 and 5 μH for a 54- and 116-inch wire length, respectively (ref. 11). Most of the literature on exploding wires (e.g., refs. 12 and 13) considers the case of a short wire (~1 in., 0.02 to 0.03 μH) fastened between two electrodes with an ignitron or other device to act as a switch. The wire inductance is small compared to the system value and, generally, the tests are conducted at room conditions. The role of driver geometry on dwell time could be an interesting subject for future research, particularly as a means of heating a gas (see, e.g., ref. 14).

Arc Discharge

Following the dwell period, the current starts to rise and its waveform is nonoscillatory as noted in figures 7 and 8. The voltage decays from its preset value to a value insufficient to support the arc column (designated as the arc-out voltage). The 54-inch arc extinguished about 165 μsec after the current had risen to 10 percent of its peak value. With a 116-inch arc, the corresponding time interval was about 325 μsec. For each arc length, the peak current was found to be closely related to the voltage drop (i.e., preset voltage minus arc-out voltage) as shown in figure 9. This figure represents a summary of over 300 tests. The cross symbols for each arc length cover a wide range of initial pressure loadings and preset voltages as noted in table I. Also tabulated in table I is the variation in conditions within the driver chamber after the arc discharge. The current-voltage relationship was not significantly affected by the gas pressure, nor, as will be discussed later, by different types or compositions of the driver gas or the trigger wire material. For all the arrangements represented in figure 9, the transfer of the bank energy to the driver was quite repeatable.

It is interesting to note the large reduction in peak current for the longer arc. Operating at lower current reduces the internal mechanical forces of the capacitors and increases the life expectancy of the capacitor bank. A lower peak current is also indicative of increased damping. The current waveforms confirm this trend. In both instances, the arc discharge is overdamped, with the longer arc the more overdamped. The increase in the degree of damping, together with the change in peak currents, allows a certain amount of speculation regarding the arc resistance. If it is assumed (in the limit) that the circuit resistance is entirely that of the arc and that it varies proportionately with the length of the arc path, then the ratio of peak currents of the 116-inch arc to the 54-inch arc would be expected to be about 0.47, the ratio of their strike distances. For the slopes of the curves shown in

figure 9, this ratio was found to be close to 0.50, which is considered good agreement and which indicates, in fact, that the arc resistance is relatively large compared to the remainder of the system.[1] By convention, the arc resistance is defined as the ratio of the potential difference to the peak current. On this basis, the arc resistance was found to decrease slightly with an increasing potential difference, varying from 15 to 11 mΩ/ft of arc length for the 116-inch arc and from 22 to 14 mΩ/ft for the shorter arc length. It was noticed that the arc resistance calculated on the basis of the slope of the curves of figure 9 was essentially constant with a value of voltage/current per foot of arc length of 10 to 11 mΩ.

A knowledge of the arc resistance is helpful in solving the RLC series circuit equations to determine the performance of a capacitor discharge into a load device. Since the capacitors used in the bank were not rated for a voltage reversal, it was necessary that all discharges be at least critically damped (nonoscillatory). Since the calculated resistance for critical damping of this energy system is 28 mΩ, the shortest arc strike necessary to assure a damped discharge would have to be about 2 feet. The corresponding peak current would be of the order of 10^6 A for an energy density of about 250 J/cm^3.

No difficulties were experienced in drawing a 54-inch arc in a helium atmosphere for preset voltage from 40 to 18 kV (fig. 10). At 16 kV, the arc strike was intermittent and no further effort was made in this regard. The arc-out voltages were relatively independent of the initial preset voltages. The duration of the arc discharge at first remained relatively constant as the preset voltage was decreased (as noted in fig. 10(b)), but below about 20 kV, the duration increased markedly. Typical current waveforms for the two conditions are illustrated in figures 10(c) and 10(d). Note also the increased dwell period in the latter figure. For the 116-inch arc, the arc strike was sporadic below 34 to 36 kV, and all tests were made with a preset voltage of 40 kV. The arc-out voltages were of the order of 16 to 20 kV. On the basis of the test results, the minimum voltage required to induce an arc strike of a given length was about 3.5 kV/ft. However, for repeatable operation, a higher value of about 3.8 kV/ft is recommended.

The arc should be completely extinguished before the diaphragm starts to open in order that the energy transfer to the driver gas be meaningful. In this regard, the diaphragm is considered an important part of the driver system. The start of the diaphragm rupture ("first light") was determined by a photomultiplier viewing upstream from a port located in the driven tube just downstream of the diaphragm. The hot driver gas serves as the source of light emission. Monitoring measurements taken simultaneously with the current history showed that the first light signal occurred about 90 μsec after the arc strike was completed. Several measurements also were made to detect a lobe of the diaphragm making contact with an insulated contact wire mounted on the wall. Opening times of approximately 135 μsec were measured for a 1/8-inch-thick stainless steel diaphragm scored from 30 to 50 percent of its depth.

---

[1]The calculated resistance of the system exclusive of the load is about 2 mΩ.

DRIVER GAS EFFECTS

The arc-out voltages measured for the two arc lengths were high with helium as the driver gas. The extinguishing voltage corresponded to about 1.8 kV/ft of strike distance and was independent of the initial loading pressure (table I). High residual or arc-out voltages are undesirable since they represent the portion of the stored energy, $(1/2)CV^2$, not discharged from the capacitor bank. To improve the bank discharge, several tests were made with different driver gases. Adding dry air to helium did not change the arc-out-voltages. With nitrogen or helium-argon mixtures, the capacitor bank potential went to zero, indicating a complete energy discharge. Representative voltage-current records are shown in figure 11. The peak current and voltage drop values also followed the characteristic curves of figure 9. Unfortunately, the gases of heavier molecular weight that improved the discharge capability also reduced the sound speed of the driver gas. This latter parameter determines the stagnation enthalpy in a shock tunnel and, generally, such decreases are undesirable.

A surprising result was noted as the test data accumulated. Pure helium as a driver gas was not as satisfactory as a mixture of 1 atmosphere of air plus helium. This trend is shown in figure 12 for the 54-inch arc driver. Note that although the initial shock speed was greater with helium as a driver gas, the shock attenuation was more pronounced and was found to be somewhat erratic from run to run. With a driver gas mixture of helium and 1 atmosphere of dry air, the run-to-run repeatability was very good. Also, the shock velocity at the end of the tube generally was higher (i.e., a more efficient driver-driven condition).

TRIGGER WIRE EFFECTS

The trigger wire has received very little attention in the literature on arc drivers. Generally, it has been considered an impurity in the driver gas and, by rule of thumb, kept to a mass less than about 1 percent of the gas load. Its purpose is to start the arc process and, hopefully, to give a complete discharge of energy from the capacitor bank over the range of initial pressure loadings of interest (ref. 15). Toward this goal, a number of wire sizes and materials (table II) were tried in the driver with a 54-inch arc length. In evaluating wire performance, circuit changes are of interest, but from a practical standpoint, a most important consideration is the net effect on the incident shock wave and its attenuation along the driven tube. All the wires were tested under the same initial driver and driven tube conditions as noted in figure 13.

Type of Material

A tungsten, chromel-C, nickel wire or a nickel foil used as the trigger wire resulted in an arc discharge. Copper, manganin, or 302 stainless steel wires did not. A 0.010-inch-diameter aluminum wire drew the arc

discharge, whereas a 0.005-inch-diameter aluminum wire did not. In all cases, the wires were exploded and at least two attempts were made with each wire to induce an arc discharge. Postrun examination for tests in which an arc was not struck showed two types of wire residues. With manganin, stainless steel, and the aluminum wires, many fine grains of wire material were distributed along the bottom length of the liner. However, with copper wire there was no visible residue. Only after cleaning with a dry rag was a very fine powder coating detected on the entire inner surface of the liner.

The fact that some materials induced an arc discharge and others did not is not totally unexpected. Present knowledge of the process now recognizes that all exploding wires are not the same, that is, they differ only in degree (see ref. 13). Other arc-heated drivers have experienced similar results, that is, no arc occurred with copper and sporadic arc strikes were obtained with aluminum wires (R. F. Flagg, private communication). Factors affecting the exploded wire-arc phenomena are complex and beyond the scope of this report. It will suffice to say that in the arc driver, very high energy densities were applied to the wire (of the order of 10^6 J/gm), and magnetic pressures may have played a dominant role in the wire-arc process.

Mass of Wire

Consider now the materials that culminated in an arc discharge. The ratio of the mass of the wire to the mass of helium gas varied from 0.41 to a maximum of 10.9 percent. The results are summarized in figure 13. Although the arc-out voltage decreased with increasing wire mass, the corresponding voltage drop and peak current increased. These latter values again followed the characteristic curve shown in figure 9, and the data for the several materials in table II are identified in that figure. The net effect was that the arc performance was not changed significantly by the type or mass of the trigger wire. Since the concentration of vaporized wire material, for a 10-percent mass, represents less than a 0.1-percent mole fraction of the total gas mixture, the small effects of wire size are understandable.

The preceding phenomenon was not seemingly a function of the initial current conduction (preset voltage/wire resistance) in the wire just prior to the wire explosion. For example, consider the 0.005-inch-diameter tungsten and chromel-C wires. The initial currents calculated on the basis of the resistance values in table II are 4300 and 230 A, respectively. The measured peak currents for both wires (~294 kA) were within 1 kA of each other. Thus, the resistance of the solid wire does not appear to be particularly pertinent to the wire-arc process.

The performance of the driver in terms of shock-tube behavior was not affected by the changes in wire mass. The velocity of the incident shock wave emanating from the driver was practically constant and its attenuation remained unchanged, as can be noted by comparing figures 12 and 13(b). In addition, the wall pressure histories at the end of the driven tube were indistinguishable from one another. The decreasing arc-out voltages noted in figure 13(a) are indicative of an improvement in the stored electrical energy

discharged from the capacitor bank to the driver chamber. It increased from 0.92 for a 1-percent wire mass to about 0.98 for a 10-percent mass. However, the performance of the driven tube was not really affected.

CONCLUDING REMARKS

A 1-MJ energy storage and arc-heated helium driver system has been developed that can operate over a wide range of conditions and is thus suitable for driving a variety of test facilities for gasdynamic and gas physics investigations. Operation with arc lengths of 54 and 116 inches in a cylindrical chamber has been demonstrated. With reasonable safety precautions, the system did not present any serious operational problems. The arc discharge was found to be consistent and reproducible for preset voltages ranging from 18 to 40 kV using a simple triggered gap switch.

The current-voltage relationship of the arc discharge was found to follow a characteristic curve for each arc length that was not affected significantly by the initial pressure of the driver gas, by different gases, or by the trigger wire material. Tungsten, chromel-C, and nickel foil wires initiated an arc discharge; copper, manganin, and 302 stainless steel wires did not induce an arc strike. It may be asked why some wires were satisfactory and others were not. This question cannot be answered conclusively. The interrelationships of the dynamics of the fast exploding wire regime, the action of the plasma at high magnetic pressures, and the radiation transfer mechanisms are formidable problems that require further investigation.

The performance of the driver in terms of shock-tube behavior was not affected by changes in the mass of the trigger wire.

Ames Research Center
National Aeronautics and Space Administration
Moffett Field, Calif. 94035, Dec. 27, 1968
129-01-03-03-00-21

APPENDIX A

SYSTEM DESCRIPTION

The energy storage and driver system consists of the following major subsystems: (1) a 40-kV, 1-MJ capacitor bank, (2) a constant dc power supply, (3) control, capacitor discharge, and capacitor shorting equipment, and (4) a driver tube. Overall views of the driver area and capacitor room are shown in figures 1 and 14.

Capacitor Bank

The energy storage system is a capacitor bank consisting of 180 capacitor units, each rated at 27.5 μF for 20 kV dc. The capacitors are individually fused by 20-kV fuses and are bussed into 10 groups of 18 capacitors each. A schematic wiring diagram is shown in figure 15. The case studs of all capacitor units are bussed together even though the rack structure also serves as a common bus for all units. A removable link connects the paralleling bus for 9 of the fused units in each group to a copper plate (fig. 16) that serves as a termination for the center conductors of two RG-17 cables, while the other 9 fused units in that group are connected by another removable link to a plate that serves as a termination for the RG-17 cable shields. Each group forms a series pair for operation at 40 kV. The rack structure is mounted on 95-kV, standoff insulators.

The removable links serve as a switchover from maximum energy-storage capacity to 90, 80, 70, 60, 50, 40, 30, 20, or 10 percent capacity and allow the system to operate at rated voltage. This arrangement also permits "hipot" testing of the driver collector assembly and cabling as part of the routine preventive maintenance of the system.

A discharge resistor network located in the capacitor room is connected by a vacuum switch and an RG-17 cable to the collector ring assembly on the driver. The network is used for "dumping" any residual bank energy after a test, or in the event of an aborted test. The discharge network is supplemented by air-operated, individual capacitor shorting switches that operate only after the bank has dropped to less than 10 V. Figure 17 shows the arrangement of the bus bars, fuses, shorting switches, shorting rods, and air cylinders. On the opposite end of the shorting bars (fig. 18), semaphore arms visibly indicate the status and actuate limit switches for remote status indication.

High-Voltage Power Supply

The capacitor charging equipment is a constant current (0.84 A), solid-state, high-voltage power supply operating from a 208 V, 3-phase, 60-cycle power source. The final output voltage is selectable over a 0 to 40,000 V range by means of an adjustable, set-point meter relay on the system control

panel. The high-voltage output from the power supply is connected through a length of RG-17 coaxial cable to the collector assembly on the driver and from there to the capacitor bank via two RG-17 cables per group of 18 capacitors. Rack (capacitor bank midpoint) voltage is connected to a resistive voltage divider in the power supply for application to a circuit that will automatically abort the charging cycle in the event the rack voltage differs more than about 500 V from half the power supply output voltage.

Controls

The control subsystem is designed to provide maximum safety for the operator and essentially automatic operation of the charge-discharge cycle. An interlock system prohibits the application of the charging voltage unless the proper pattern of system checkout from the capacitor room through the control room is followed.

In addition to the control panel meter relay that permits presetting and monitoring of the bank voltage during charging, the system includes a resistive voltage divider and a capacitive voltage divider from the capacitor midpoint (rack structure) to ground. The former is used to monitor the complete charge-discharge cycle by means of a strip chart recorder. The capacitive divider output, which is recorded on an oscilloscope, is used to monitor the driver high-voltage electrode signal during discharge.

A current shunt is used to monitor the portion of the discharge current flowing in one capacitor group by measuring the voltage drop along the known ground return resistance (shields of the cables in parallel). The total discharge current is equal to the current flowing in the cable return multiplied by the number of capacitor groups, since all the coaxial cables are of equal length (46.5 ft) and all capacitor groups are symmetrical.

Driver

A schematic assembly of the driver is shown in figure 4. The driver tubes were machined from type A286 austenitic (nonmagnetic) stainless steel forgings and have a 4-3/4-inch inside diameter that accommodates an insulating liner of wound fiberglas whose bore is coated with RTV silicone rubber. The final arc chamber is 4 inches in diameter with a maximum length of about 10 feet. The heavy flanges at the downstream ends of both driver tubes incorporate a removable insert that can hold the diaphragm section. The arc-strike distance from the high-voltage electrode to the spider electrode is 116.3 inches for the assembly shown in figure 4. When the spider and diaphragm are mounted in the upstream end of the forward tube, the arc-strike distance is reduced to 54.2 inches. The arc length can be reduced to as little as 18 inches by the use of shorter liners together with a longer Lexan filler plug and electrode. At the downstream end of the driver is a copper electrode on a stainless steel spider to which the arc-initiating wire is attached (fig. 19). The complete system is also connected to earth ground at this flange by means of a heavy flexible braided ground strap. Downstream of the diaphragm, a 4-inch-square to 4-inch-diameter transition section provides for gradual

transition into the tube diameter (fig. 20). Flat scored diaphragms are used. They are fabricated in different thicknesses (1/16 to 3/8 in.) and are scored from 30 to 50 percent of their depth to control their bursting pressure. The diaphragm material is hot-rolled, fully annealed type 321 stainless steel, which has been found to produce consistent lobe formations without fragmenting (ref. 16).

The high-voltage electrode assembly is brought into the arc chamber through a quarter-turn stainless steel breech plug. The electrode is electrically insulated from the breech plug by Lexan insulating elements (fig. 21). The current collector assembly, which provides a common point for tying the coaxial power cables from the capacitor bank, power supply, and discharge resistors, consists of two concentric cylinders separated by Lexan insulating spacers. The outer cylinder is attached to the driver tube and serves as the ground connection for the cable shields. The inner cylinder provides a termination for the center conductors of the cables and is insulated from the driver tube as well as from the electrode assembly so that the latter unit may be checked for electrical isolation before each run (fig. 22). The high-voltage assembly is checked with a hipot tester to at least 10 kV over that required for the particular run. The purpose of the check is to reduce to a minimum the chance of a structure-damaging arc-over to the driver wall or of a premature arc occurring before the proper preset voltage is attained. When these hipot tests have been made, a copper contact plate with spring fingers is bolted to the electrode assembly, connecting it to the inner collector assembly cylinder (fig. 23).

The arc is initiated by means of a fine wire attached to the spider electrode at the downstream end of the driver chamber and separated at least 3 inches from the high-voltage electrode by a short piece of cotton thread. The wire is flexed slightly on installation as its length is equal to the distance between the electrodes. The thread is attached to a firing rod that passes through the hollow core of the high-voltage electrode. After the capacitor bank has reached its preset voltage, a pneumatically operated piston (4-in. travel) causes the firing rod to pull the trigger wire toward the main electrode until a high current is initiated to vaporize the wire and thus provide a path for the arc strike.

A single RTV coated fiberglas liner has been found to be usable for at least 40 to 60 runs. After each firing, the liner and driven tube surfaces were coated with a fine black powder (the ablation products of silicone rubber). This deposit is sufficient to influence performance (shock velocity) and, for best results, the liner and shock tube are wiped clean after every run. There was no evidence of wear from the residue on the honed surface of the driven tube after over 200 firings. Other researchers have reported successful operation with ceramic liners in short drivers (see, e.g., ref. 17).

REFERENCES

1. Loubsky, William J.; and Reller, John O., Jr.: Analysis of Tailored-Interface Operation of Shock Tubes With Helium-Driven Planetary Gases. NASA TN D-3495, 1966.

2. Smith, C. E.; Hajjar, D. G.; and Reinecke, W. G.: A Study of Large, High-Performance Shock Tunnel Drivers. AFAPL-TR-67-73, AVCO, 17 July 1967.

3. Camm, J. C.; and Rose, P. H.: Electric Shock Tube for High Velocity Simulation. AFCRL-62-568, AVCO, July 1962.

4. Warren, W. R.; Rogers, D. A.; and Harris, C. J.: The Development of an Electrically Heated Shock Driven Test Facility. 2nd Symposium on Hypervelocity Techniques, Univ. of Denver, March 20-21, 1962.

5. Livingston, F. R.: Electric Arc-Driven Shock Tube Diameter, Length and Energy Requirements for the Study of Gas Radiation Phenomena. 5th Shock Tube Symposium, Silver Spring, Maryland, April 23-30, 1965, pp. 1035-58a.

6. Presley, L. L.; Falkenthal, G. E.; and Naff, J. T.: A 1 MJ Arc Discharge Shock Tube as a Chemical Kinetics Research Facility. 5th Shock Tube Symposium, Silver Spring, Maryland, April 23-30, 1965, pp. 857-78.

7. Cobine, J. D.: Gaseous Conductors, Theory and Engineering Applications. Dover Publications, New York, 1958, p. 163.

8. McDevitt, John B.; Harrison, Dean R.; and Lockman, William K.: Measurements of Pressures and Heat Transfer by FM Telemetry. IEEE Trans. Aerospace Electronic Systems AES-2, No. 1, Jan. 1966, pp. 2-12.

9. Bennett, F. D.: High Temperature Exploding Wires. Rep. BRL-R-1339, Ballistic Research Labs., Aberdeen, Maryland, Oct. 1966.

10. Fansler, K. S.; and Shear, D. D.: Correlated X-Ray and Optical Streak Photographs of Exploding Wires. BRL Rep. R-1385, Ballistic Research Labs., Dec. 1967.

11. Terman, F. E.: Radio Engineers' Handbook. McGraw-Hill, New York, 1943, p. 48.

12. Chace, W. G.; and Moore, H. K.; eds.: Exploding Wires, Vol. II, Plenum Press, New York, 1962.

13. Chace, W. G.; and Moore, H. K.; eds.: Exploding Wires, Vol. III, Plenum Press, New York, 1964.

14. Hesselgreaves, J. E.; Nonweiler, T. R. F.; and Foord, T. R.: The Heating of Air by "Dark" Discharge. British R and M, No. 3519, May 1966.

15. Mullaney, G. J.; and Ahlstrom, H. G.: The Energy Transfer Mechanism in Shock Tube Arc-Heated Drivers. FSL Report 111 (D1-82-0582) Boeing Sci. Res. Labs., Nov. 1966.

16. Dannenberg, Robert E.; and Stewart, David A.: Techniques for Improving the Opening of the Main Diaphragm in a Large Combustion Driver. NASA TN D-2735, 1965.

17. Williard, J. W.: Performance of a Ceramic-Lined 6-Inch-Diameter Arc Driver. AIAA Paper 68-366, 1968.

TABLE I.- ARC DRIVER CHARACTERISTICS

Driver designation	54 inch	116 inch
Arc strike distance, in.	54.2	116.3
Chamber void volume, $in.^3$	712	1105
Nominal I.D., in.	3-7/8	3-3/8
Range of operation		
Capacitance (180 units), μF	1250	
Preset voltages, kV	40-16	40
Initial load pressure of helium from 1 atm of air, psia	500-200	550-200
Trigger wire diameter, in.	0.005, tungsten	
Range of conditions in driver chamber after arc discharge calculated for constant volume energy transfer		
Temperature, ^{o}R	8,000/16,000	6,000/17,000
Pressure, psia	5,000/9,000	3,400/6,200
Approximate arc-out voltage, kV	8	16-20
Data point symbol, figure 9	×	+

TABLE II.- MATERIALS TESTED AS TRIGGER WIRES IN 54-INCH DRIVER

[Initial driver conditions noted in fig. 13]

Material	Diameter, in.	Resistance, Ω	Weight, gm	$\frac{\text{Mass wire}}{\text{Mass He}}$, percent
Materials for which an arc discharge occurred				
Tungsten	0.004	9.90	0.21	0.62
	.005	6.35	.34	1.00
	.007	3.20	.66	1.95
	.010	1.65	1.34	3.97
Chromel-C	.005	118.6	.14	.41
	.010	30.4	.57	1.70
	.025	4.95	3.69	10.9
Aluminum	.010	.72	.19	.56
Nickel	.008	3.96	.39	1.17
Nickel foil	0.080×.005	.58	3.15	9.3
Materials that did not induce an arc discharge				
Copper	0.003	4.72	0.06	0.16
	.0071	.89	.31	.93
302 Stainless steel	.006	60.3	.20	.59
	.010	24.5	.56	1.65
Manganin	.0031	111.3	.06	.16
	.007	32.6	.29	.85
	.018	4.0	1.86	5.5
Aluminum	.005	3.48	.05	.14

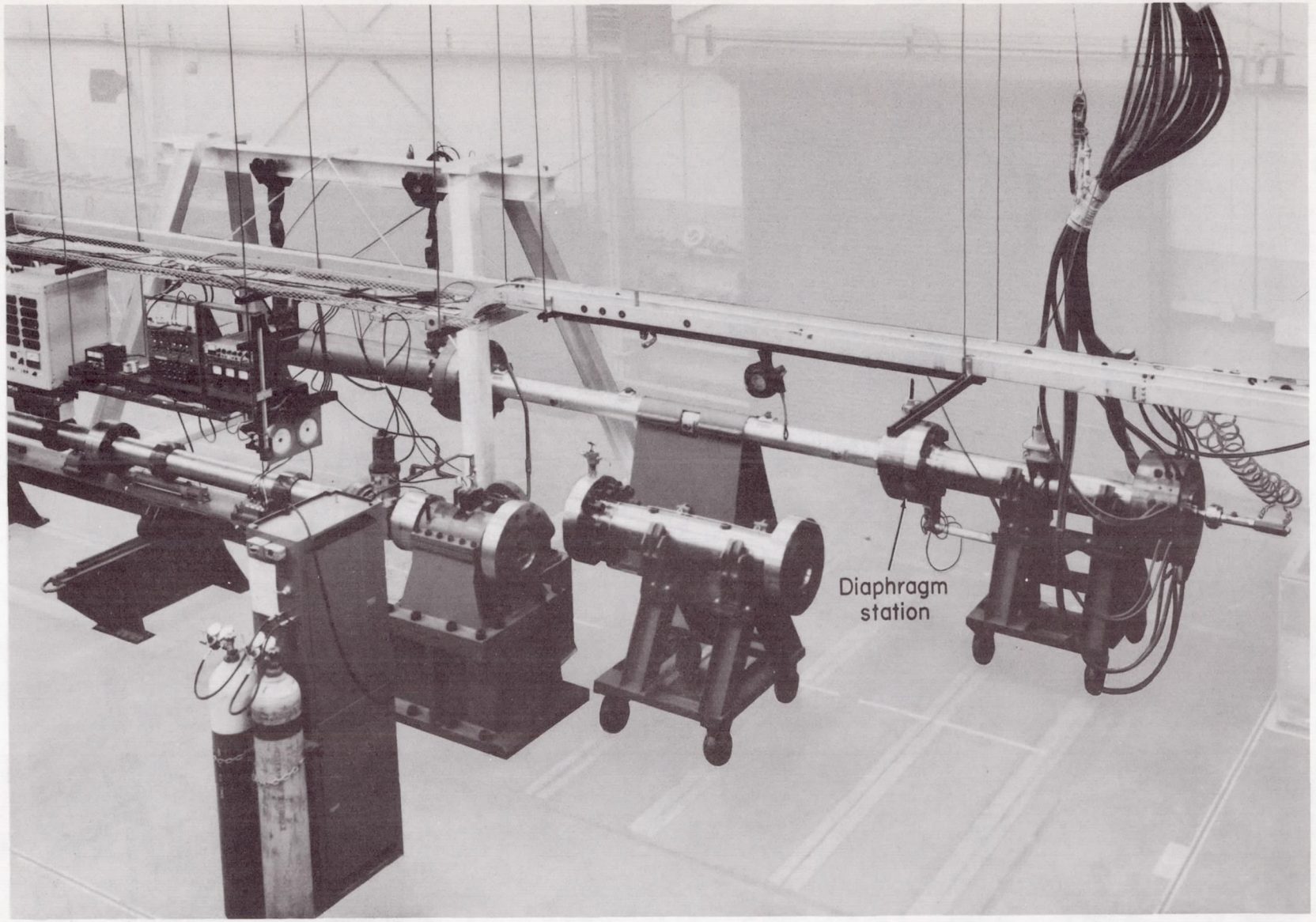

A-41455

Figure 1.- Overall view of driver area with the 54-inch arc driver in position at the diaphragm test rig.

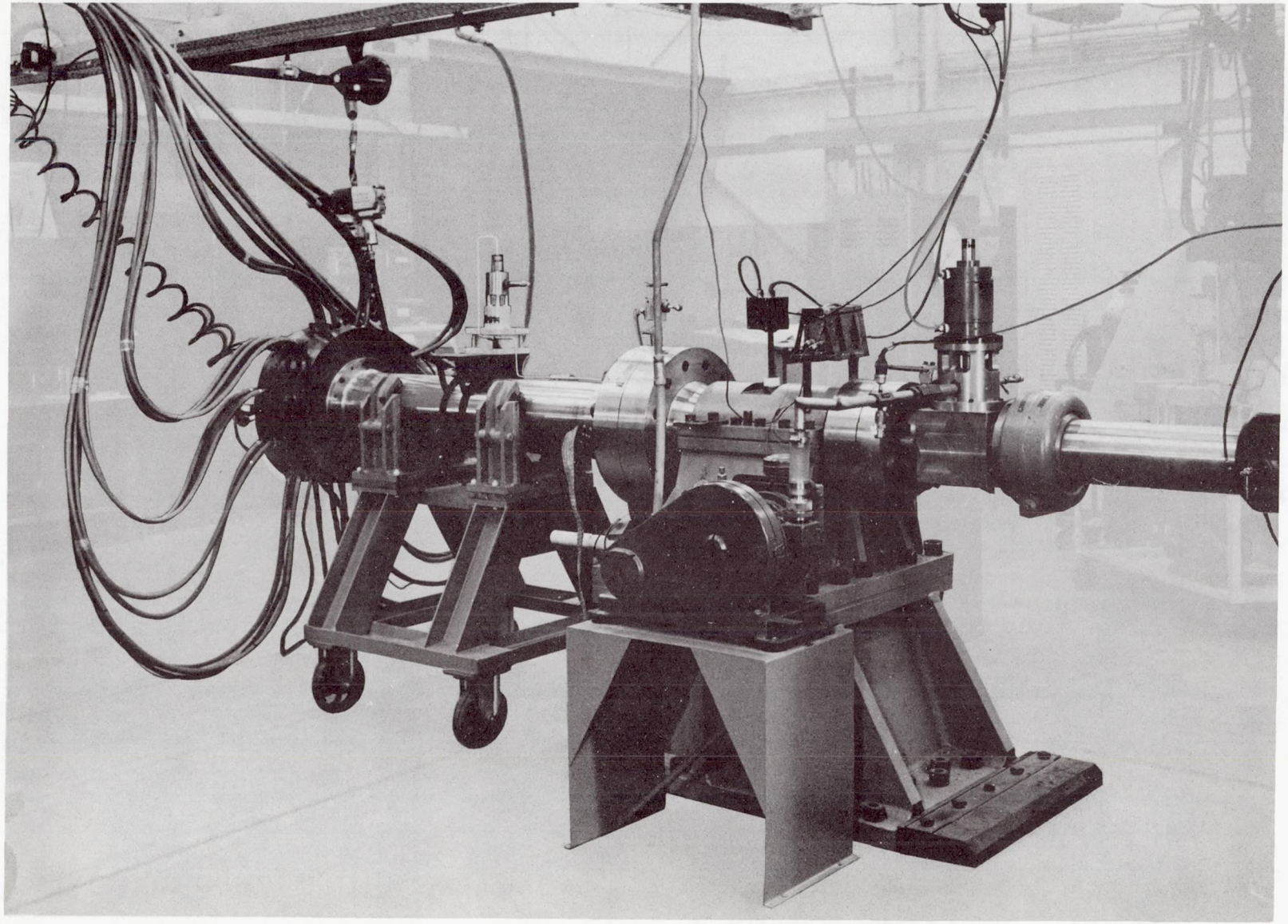

Figure 2.- The 54-inch arc driver in position at the shock tunnel station.

A-40471

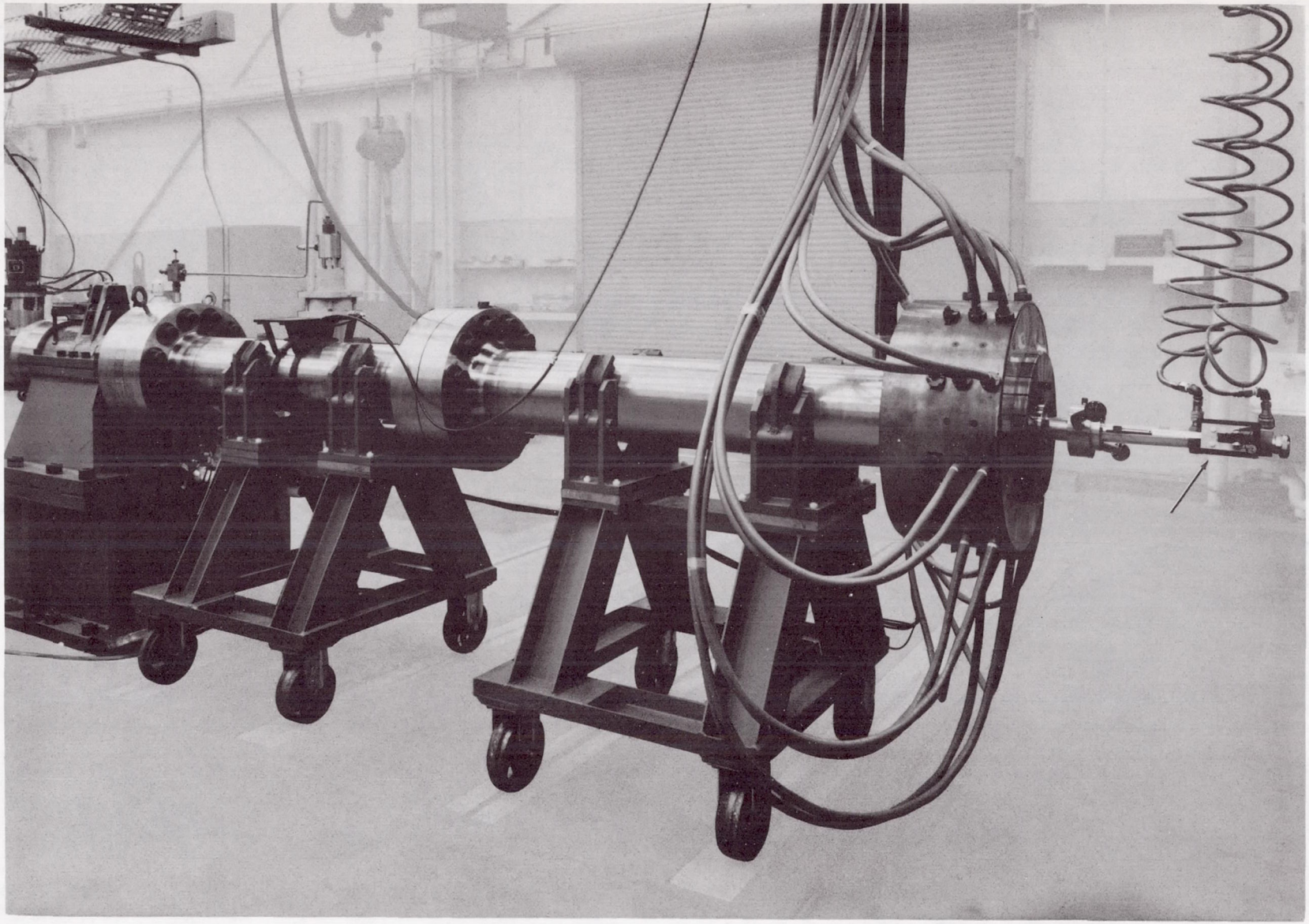

A-38602-9

Figure 3.- Ten-foot electric arc driver. Note FM transmitter on end of the air cylinder (at arrow).

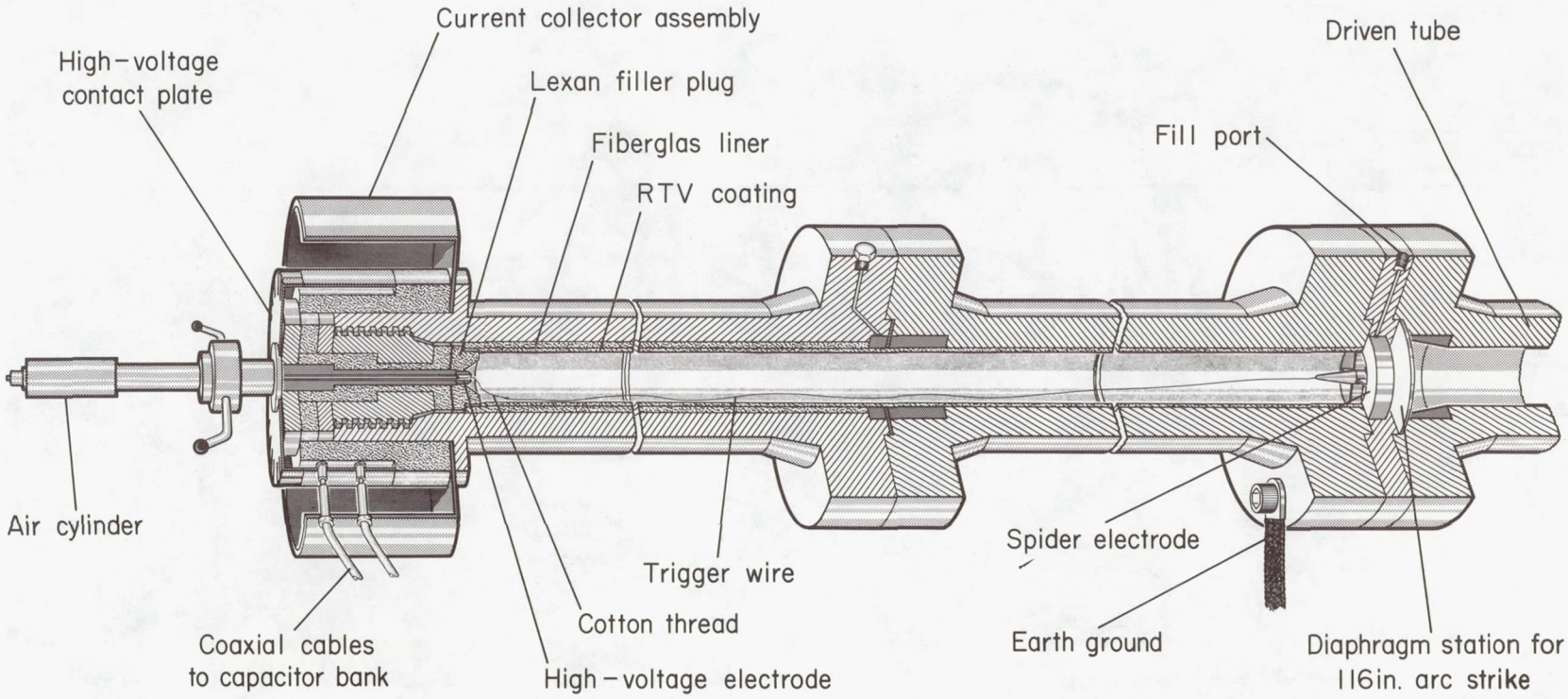

Figure 4.- Schematic assembly of electric arc driver with a chamber length of 10 feet.

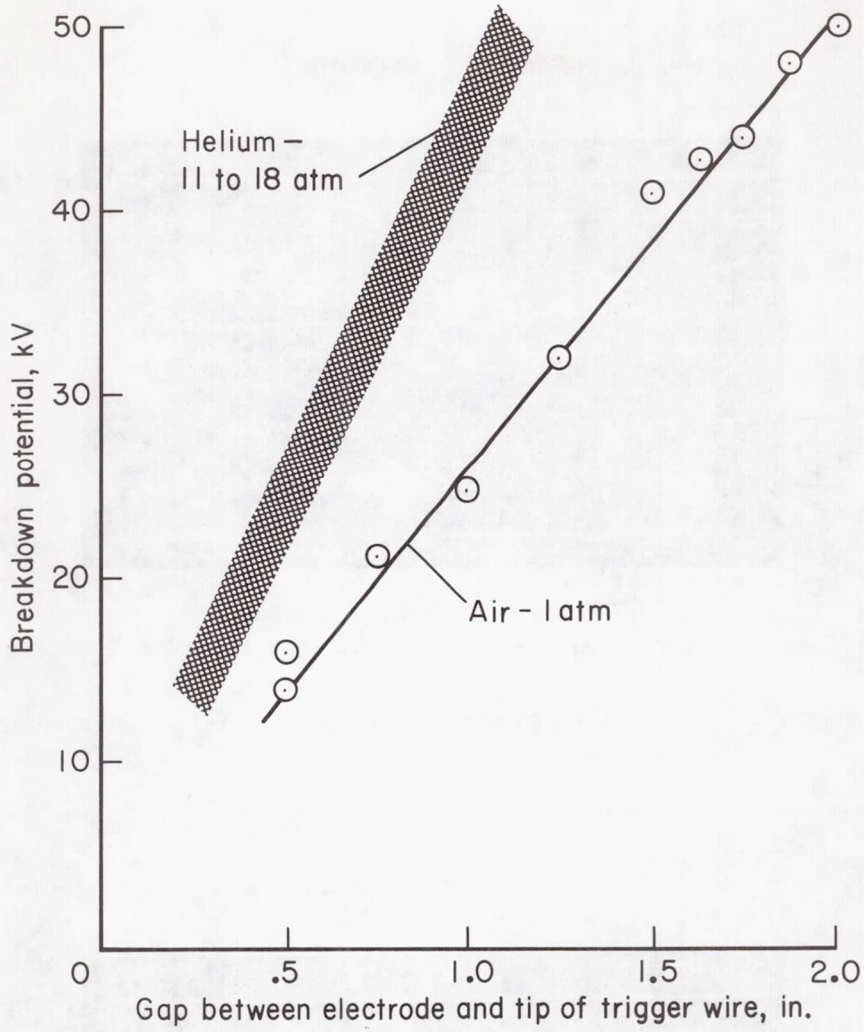

Figure 5.- Comparison of breakdown voltages for electrode-wire combination in air and helium at 70° F.

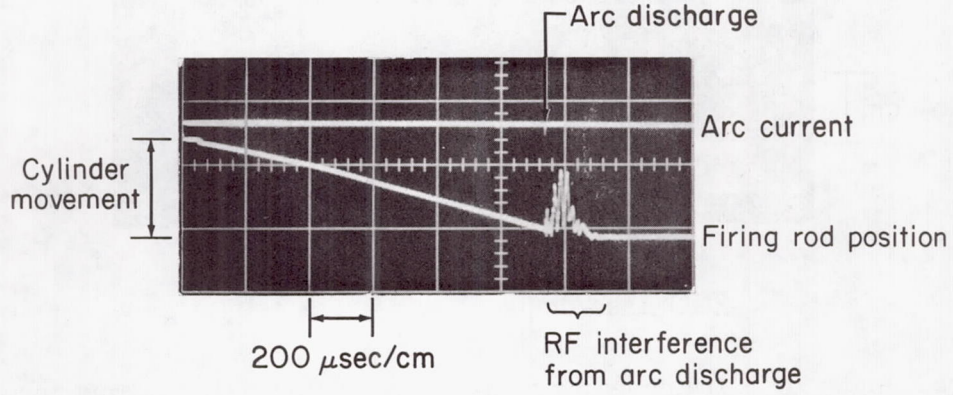

Figure 6.- Trigger wire position measurement by telemetry during an arc discharge in driver; preset voltage = 40.4 kV.

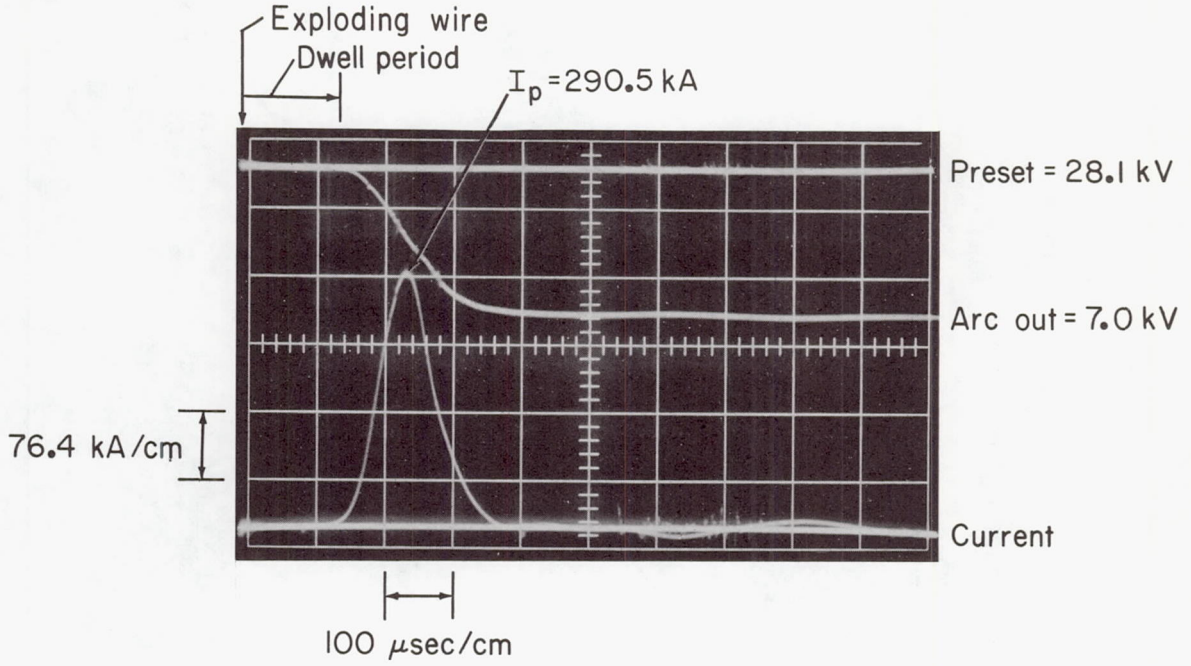

(a) Arc length of 54 inches; trigger wire = 0.005-inch-diameter tungsten.

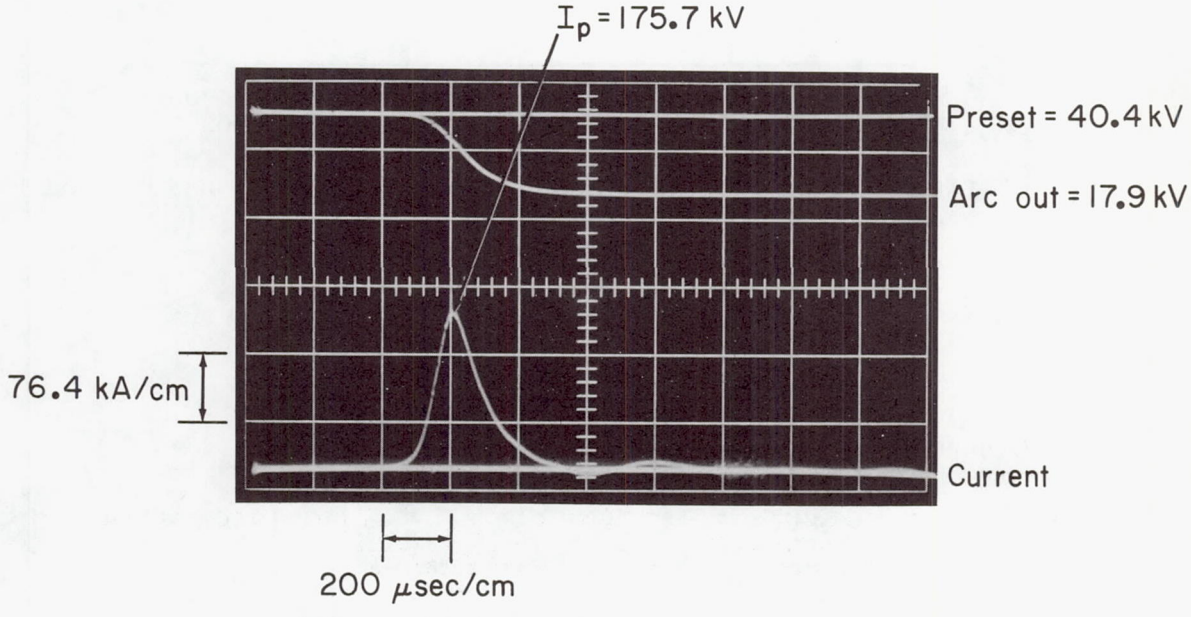

(b) Arc length of 116 inches; trigger wire = 0.005-inch-diameter tungsten.

Figure 7.- Typical electrical characteristics of the energy storage and driver system; driver load pressure of 272 psia helium.

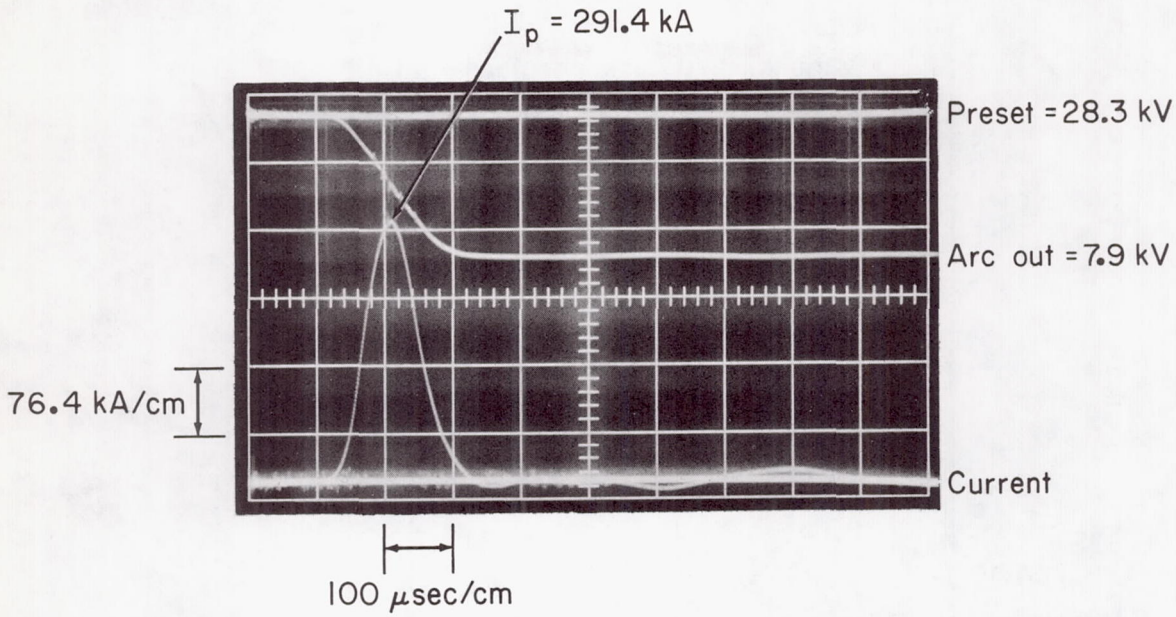

(a) Typical oscilloscope record of electrical characteristics.

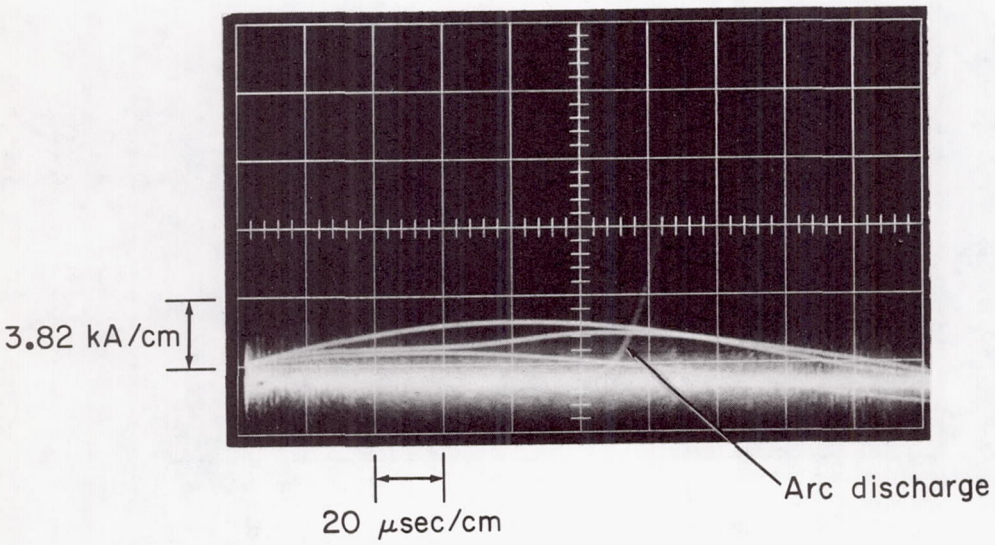

(b) Simultaneous current record with 20:1 gain and increased sweep speed.

Figure 8.- Current flow during dwell period of a 54-inch arc discharge; trigger wire = 0.008-inch-diameter nickel, driver load pressure of 272 psia helium.

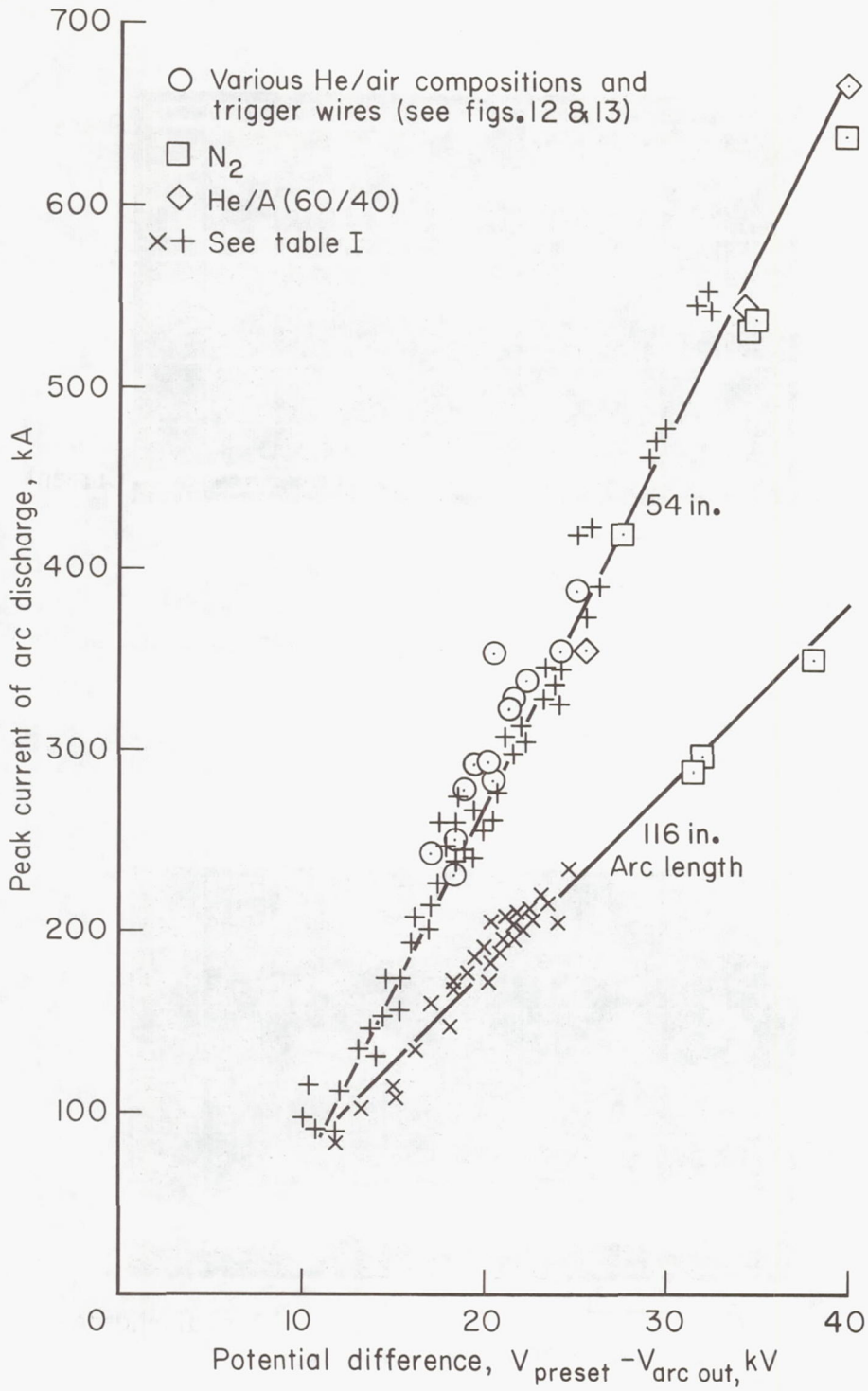

Figure 9.- Characteristic performance of system; C = 1250 μF.

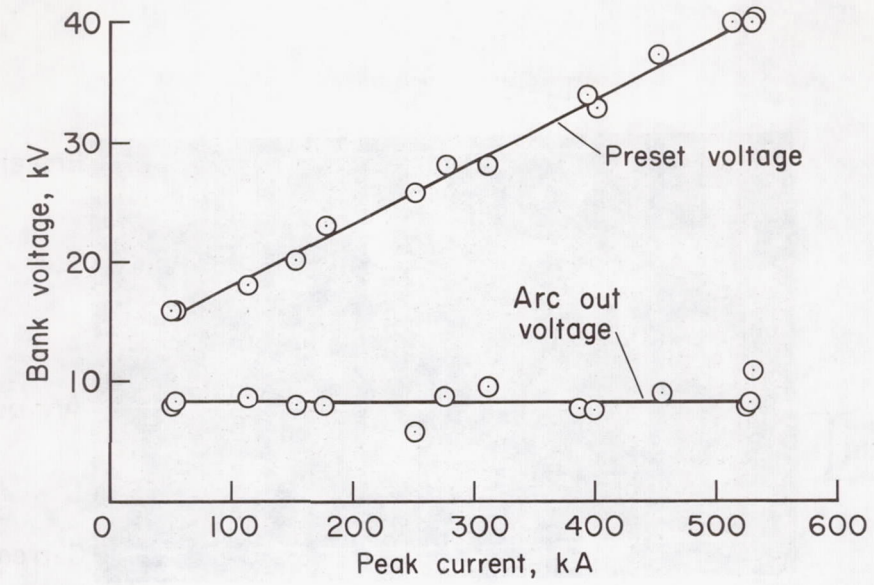

(a) Variation of preset voltage.

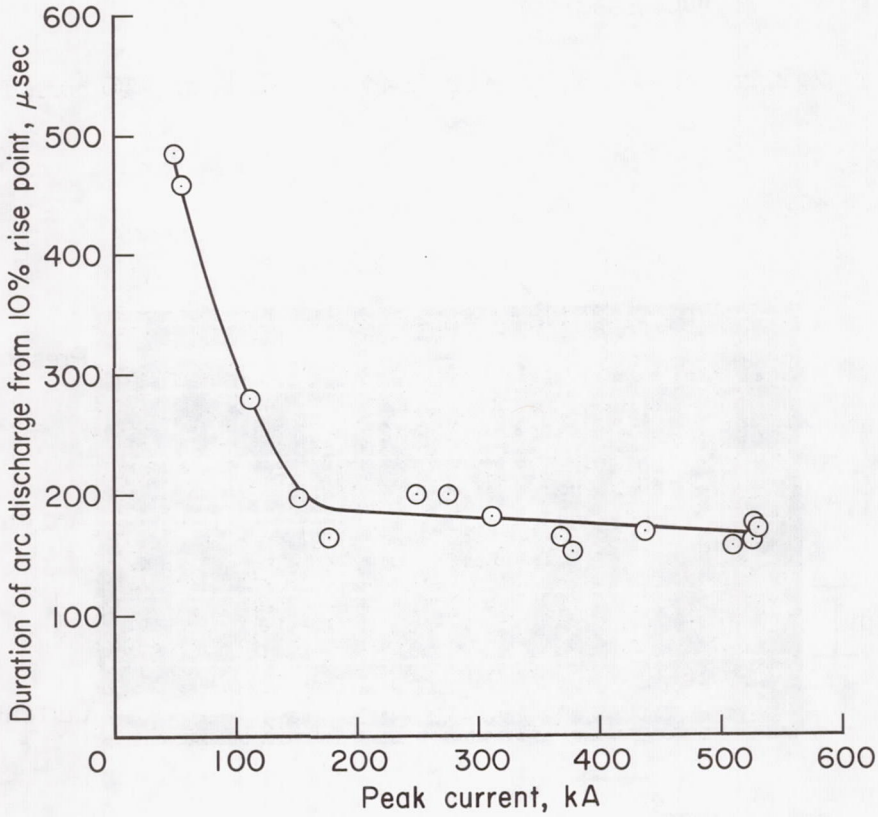

(b) Variation in duration of arc discharge.

Figure 10.- Performance characteristics of energy storage and driver system; arc length of 54 inches, tungsten trigger wire of 0.005-inch-diameter, initial driver loading pressures of 250-450 psia helium.

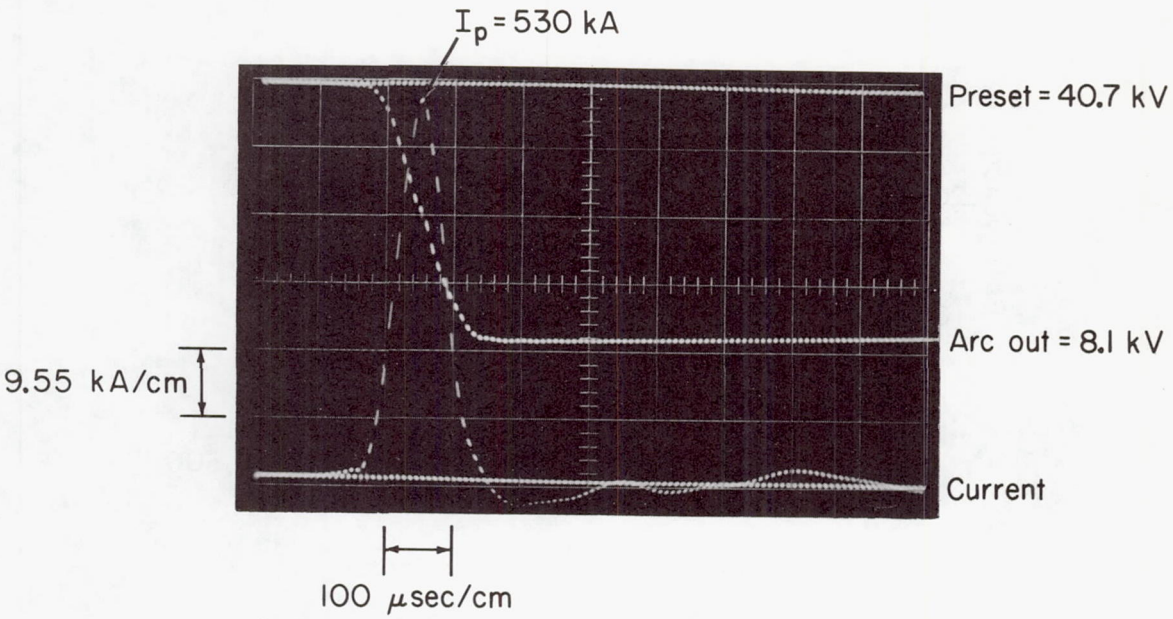

(c) Preset voltage of 40 kV; driver load pressure of 450 psia helium.

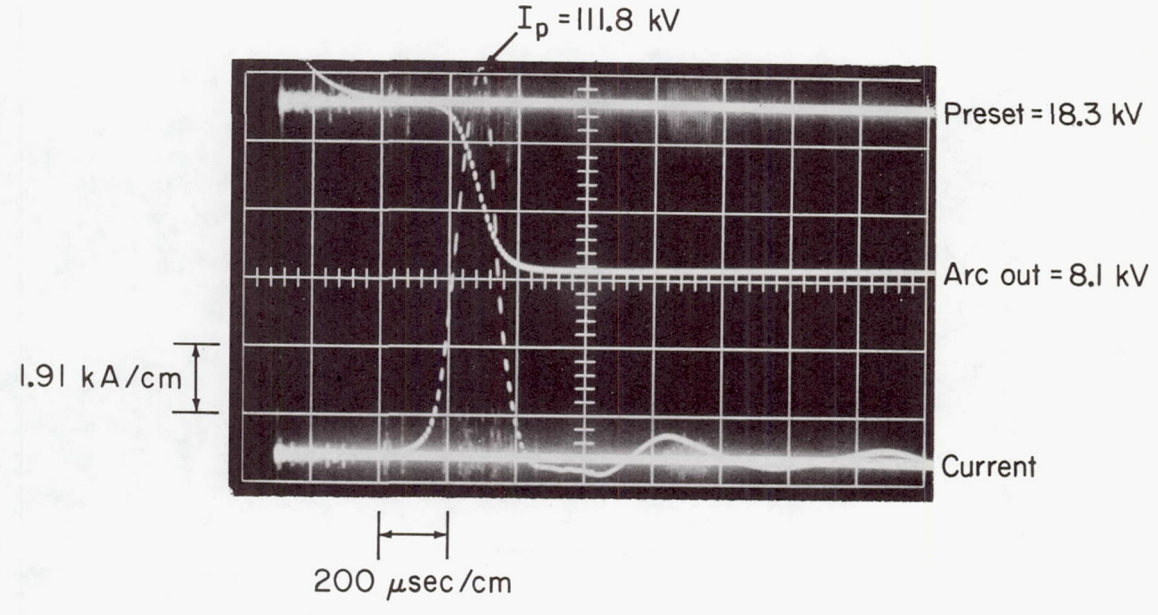

(d) Preset voltage of 18 kV; driver load pressure of 250 psia helium.

Figure 10.- Concluded.

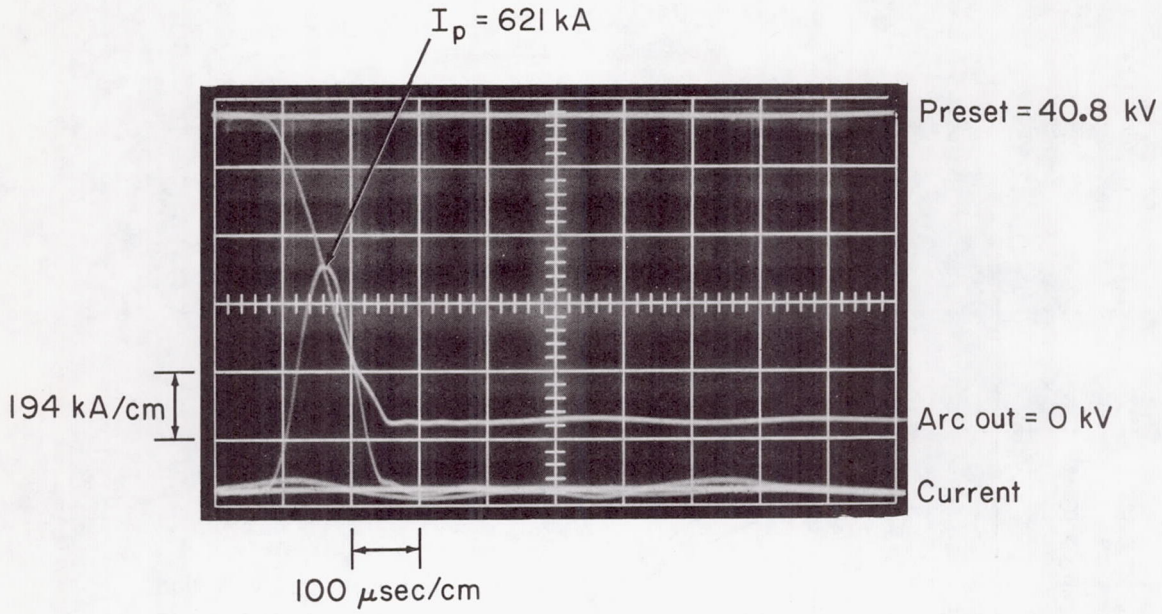

(a) Driver gas: nitrogen (see fig. 7(a) for helium).

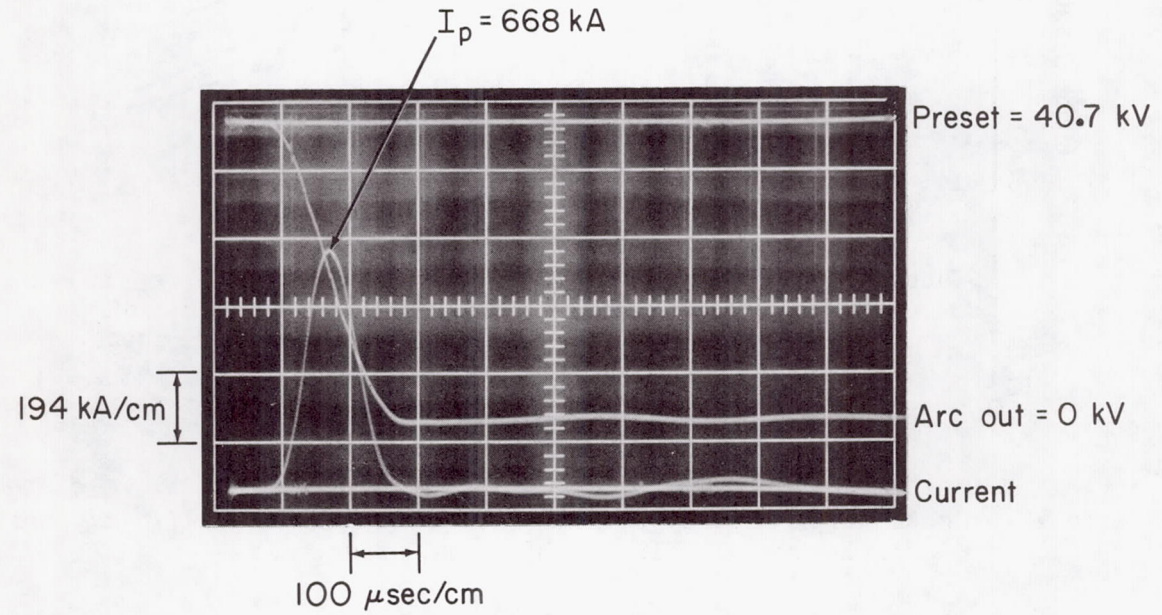

(b) Driver gas: 60/40, helium/argon.

Figure 11.- Electrical performance characteristics of the 54-inch driver with different gases; initial load pressure of 272 psia, trigger wire of 0.005-inch-diameter tungsten.

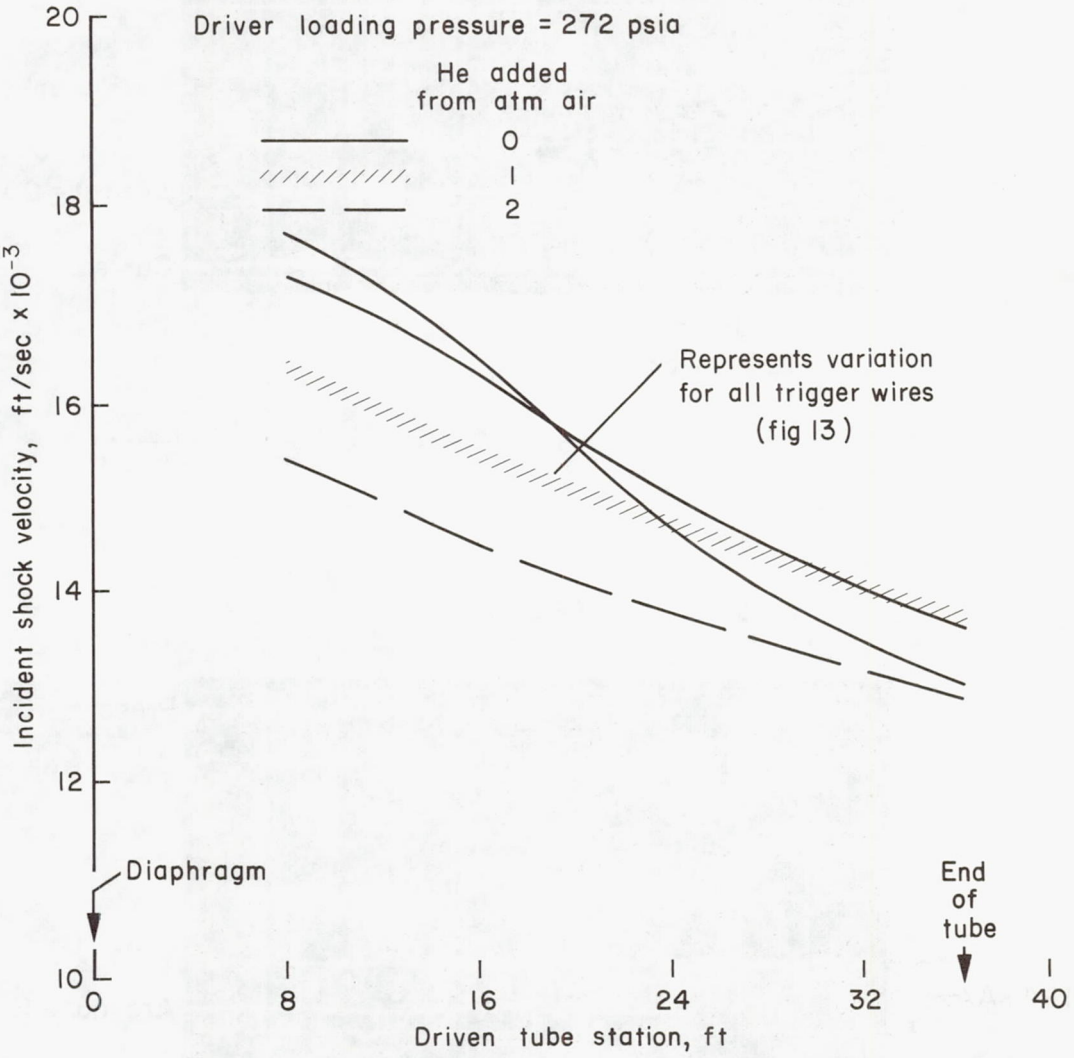

Figure 12.- Shock wave velocity profiles; preset voltage of 27.5 kV, initial driven tube loading of 35 mm Hg of dry air.

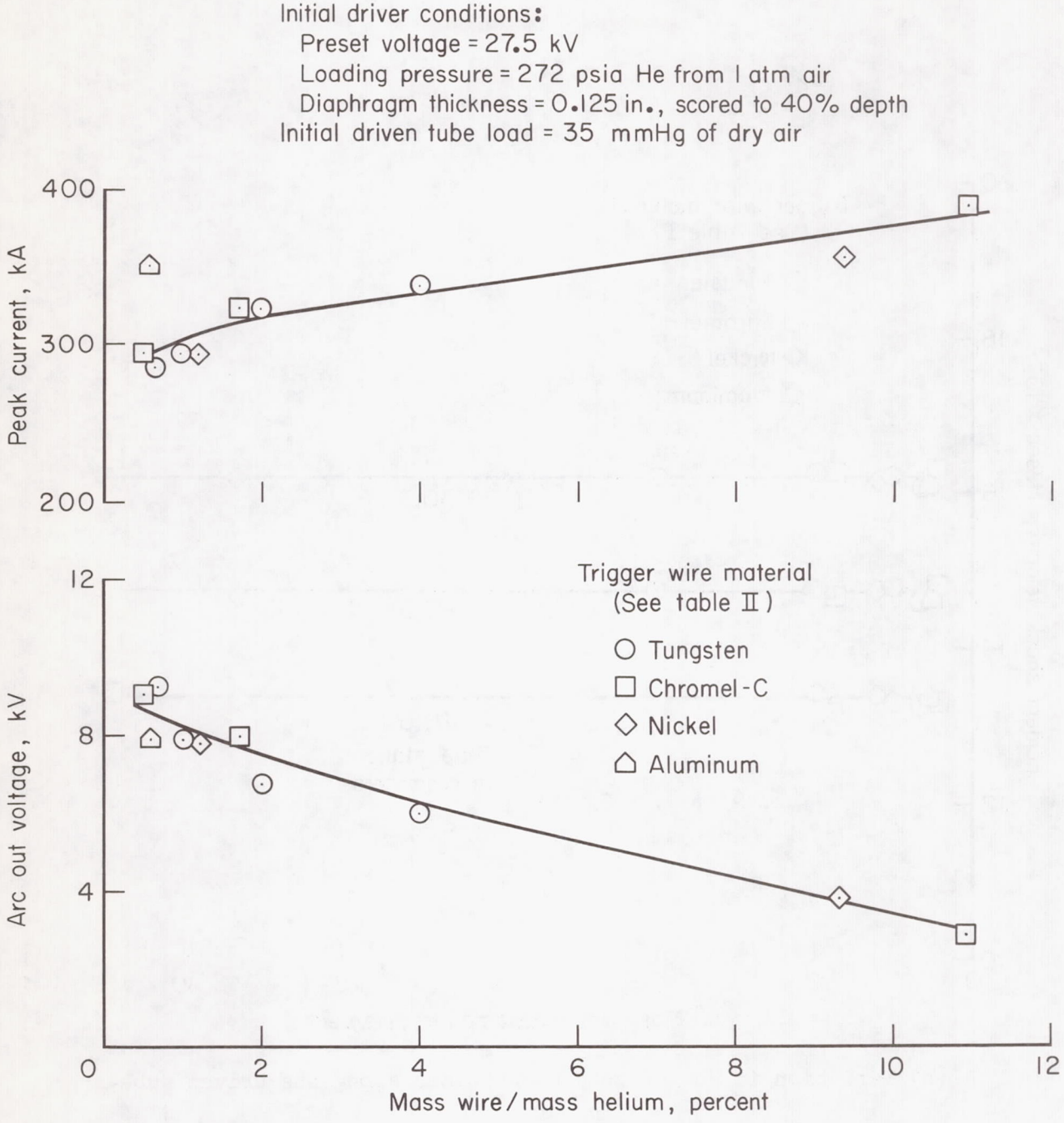

(a) Electrical characteristics.

Figure 13.- Performance characteristics of energy storage and driver system with different trigger wires used for arc initiation.

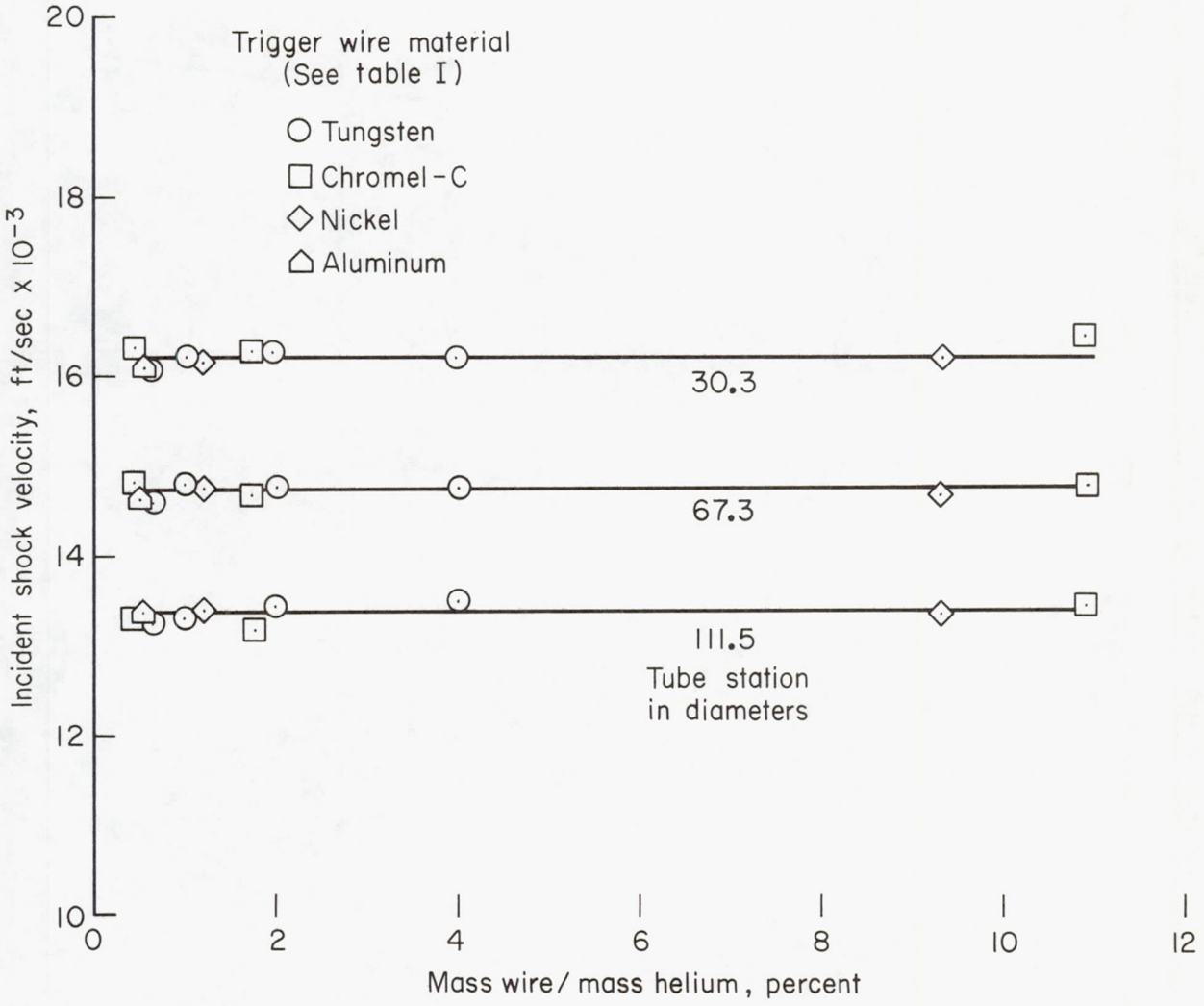

(b) Variation in shock speed at stations along the driven tube.

Figure 13.- Concluded.

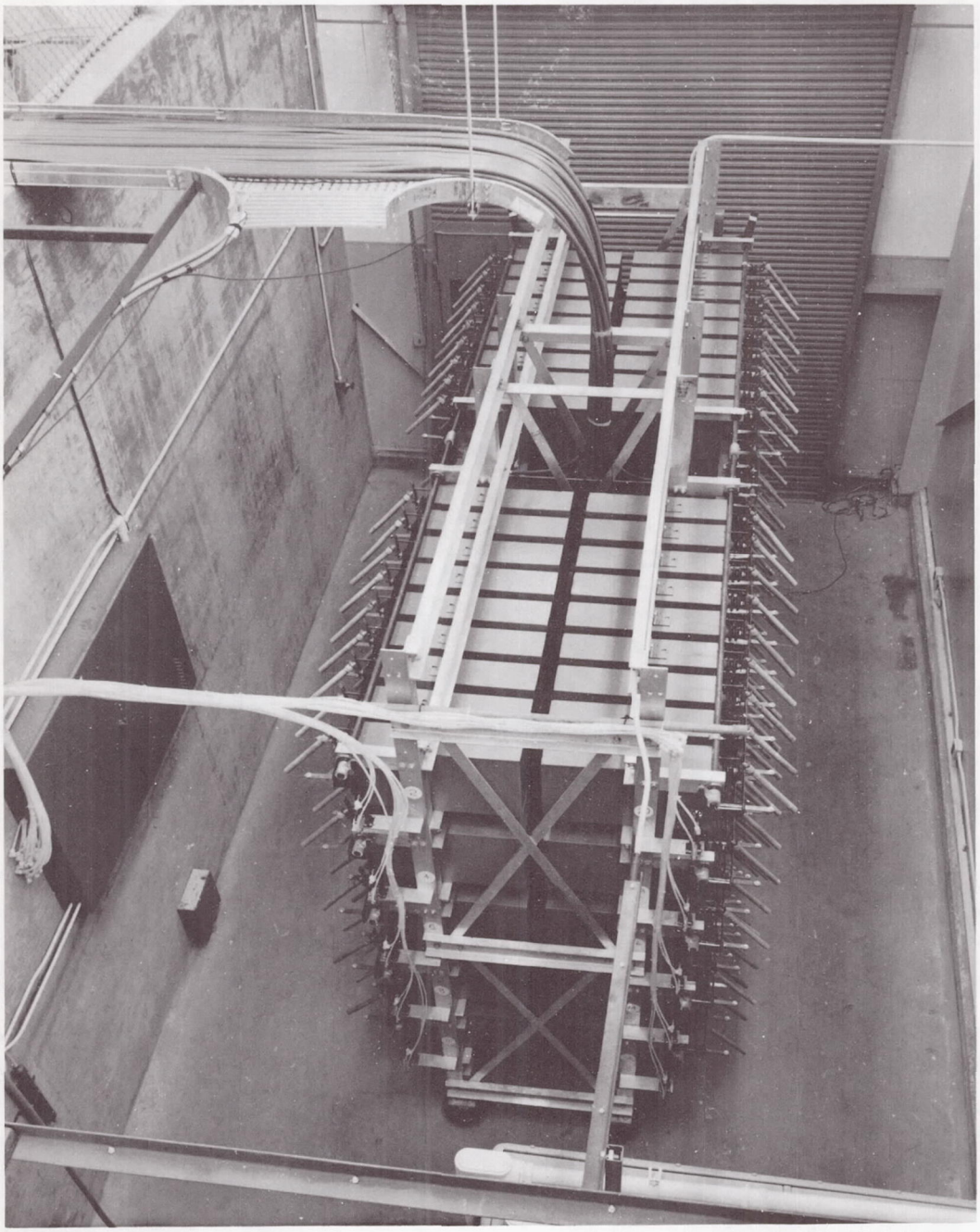

A-36587-6

Figure 14.- One megajoule energy storage bank consisting of 180 capacitor units.

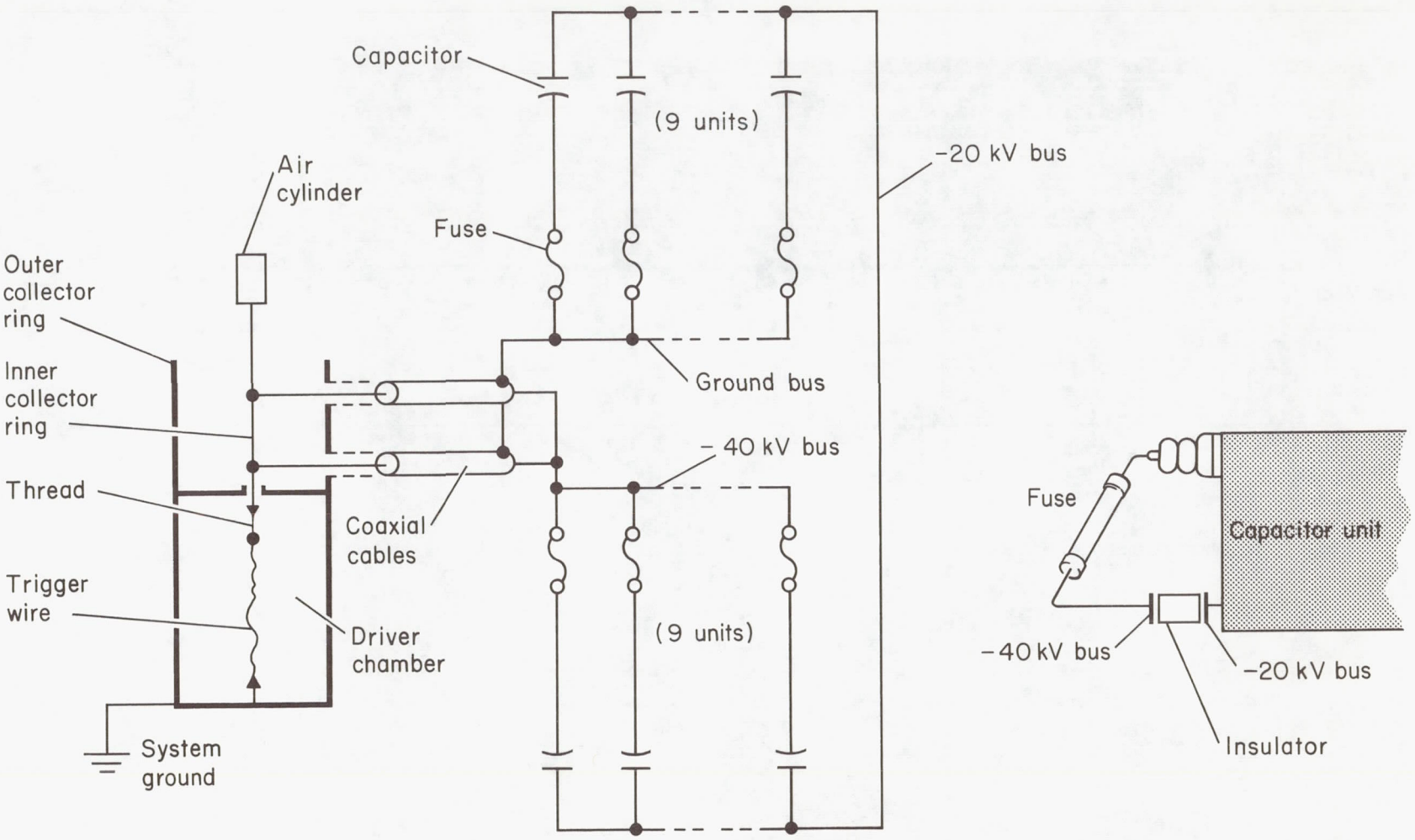

Figure 15.- Schematic diagram of one row of 18 capacitors in series/parallel; total bank of ten rows, 180 capacitors, and 20 RG-17/u coaxial cables.

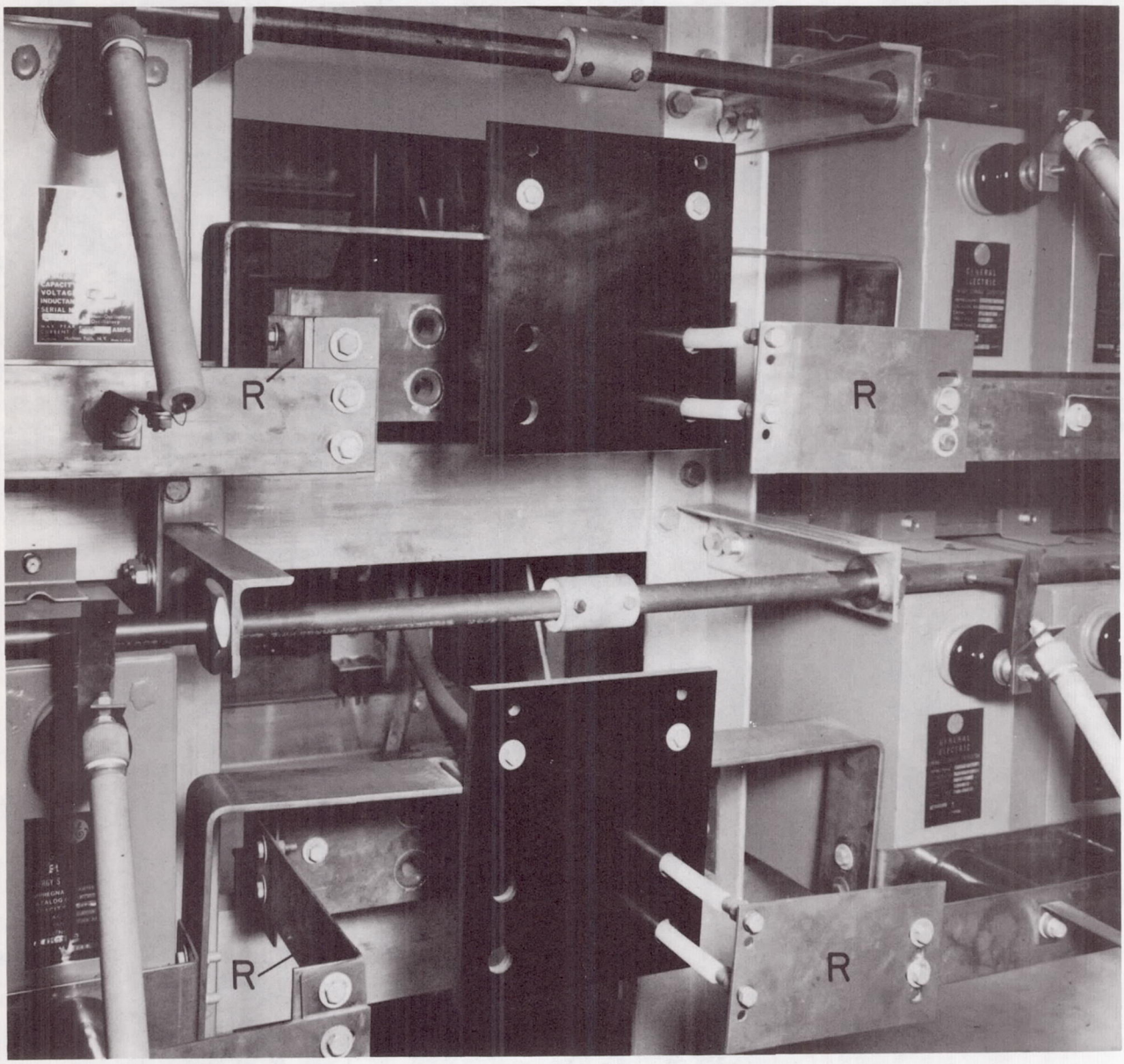

A-38602-11

Figure 16.- Detail of removable-link section of capacitor rack; removable portions are noted by R.

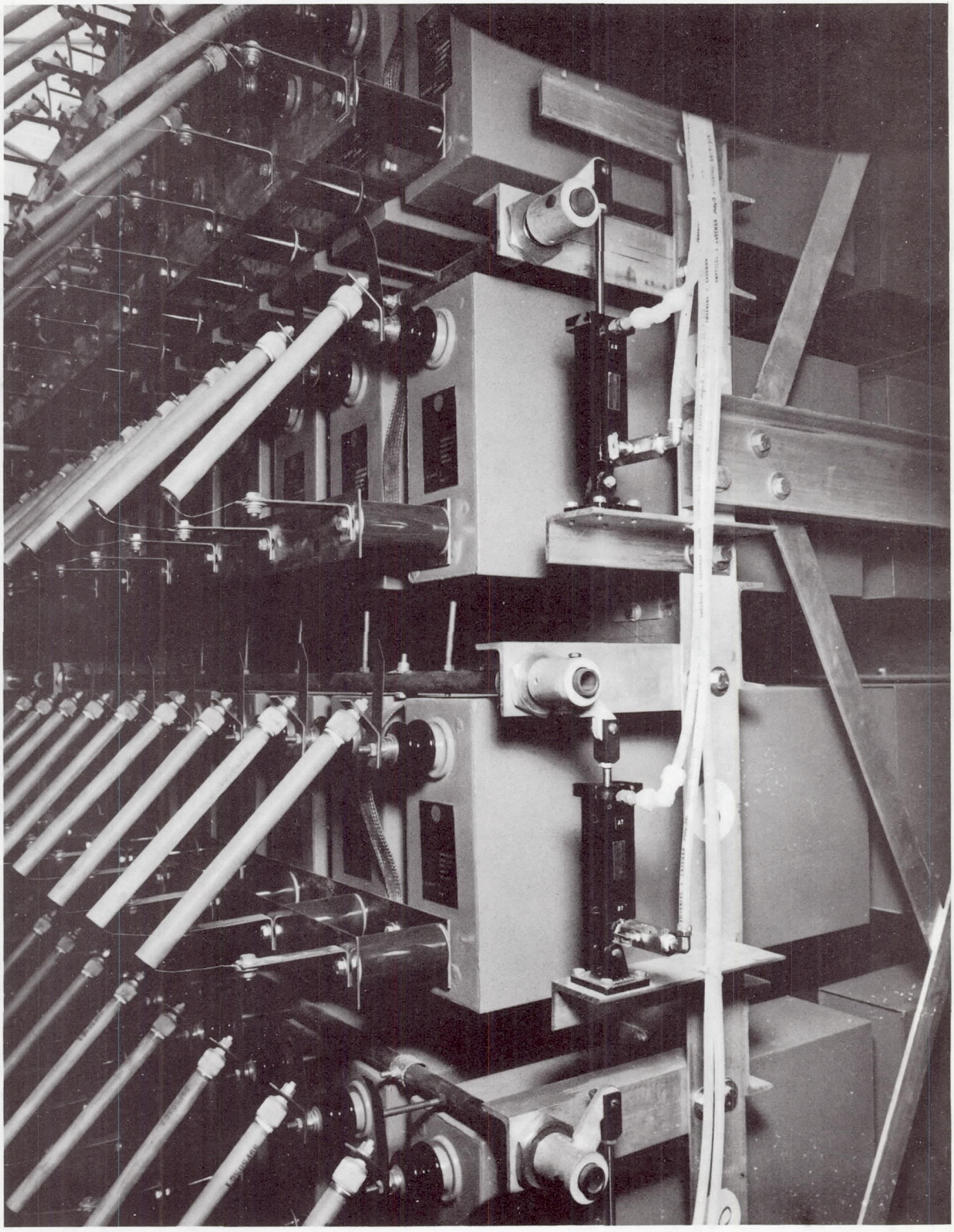

A-36587-9

Figure 17.- Detail of capacitor rack showing air operated shorting switches. Note that center row of switches is in open position.

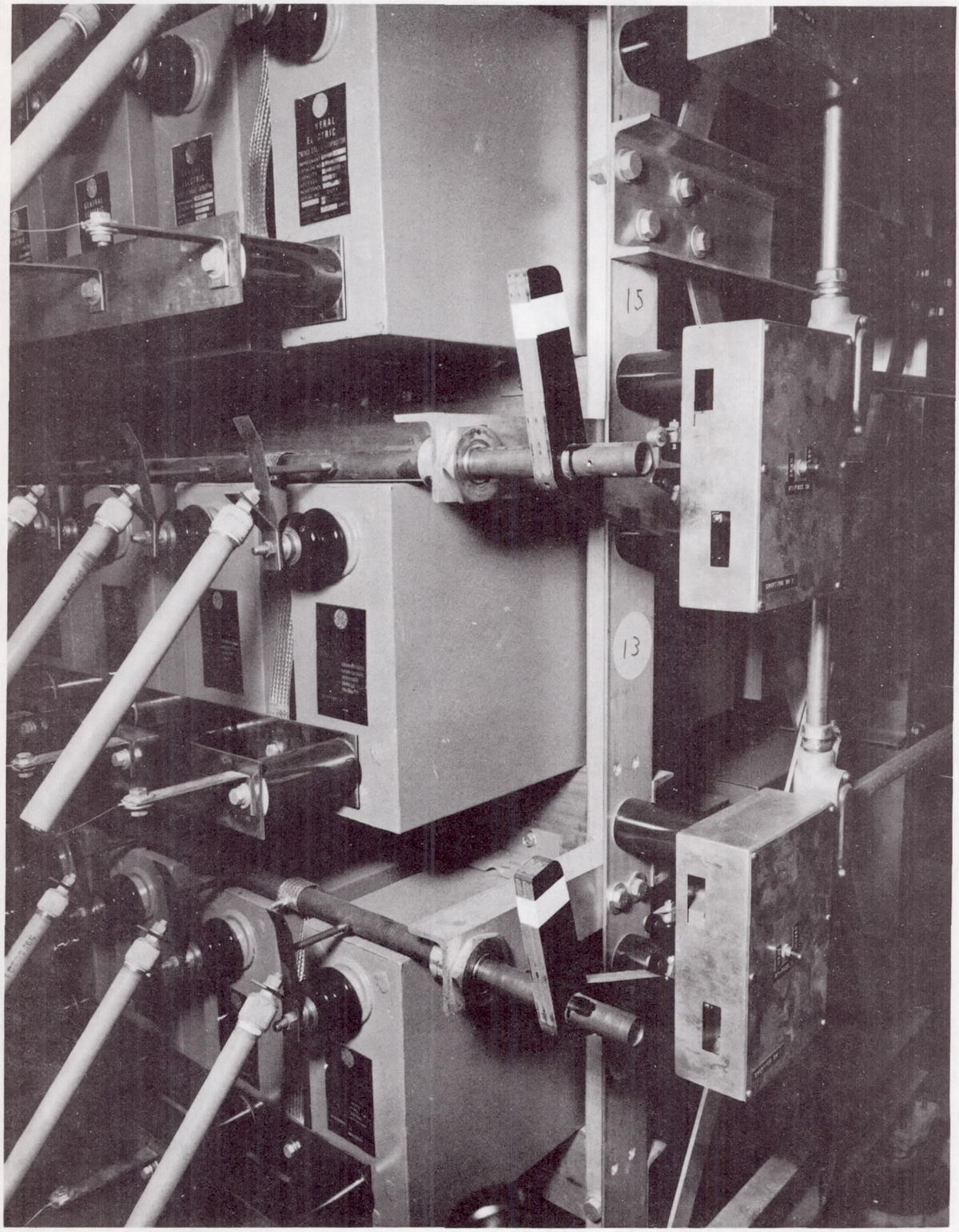

A-36587-8

Figure 18.- View of capacitor rack showing status arms and limit switches.

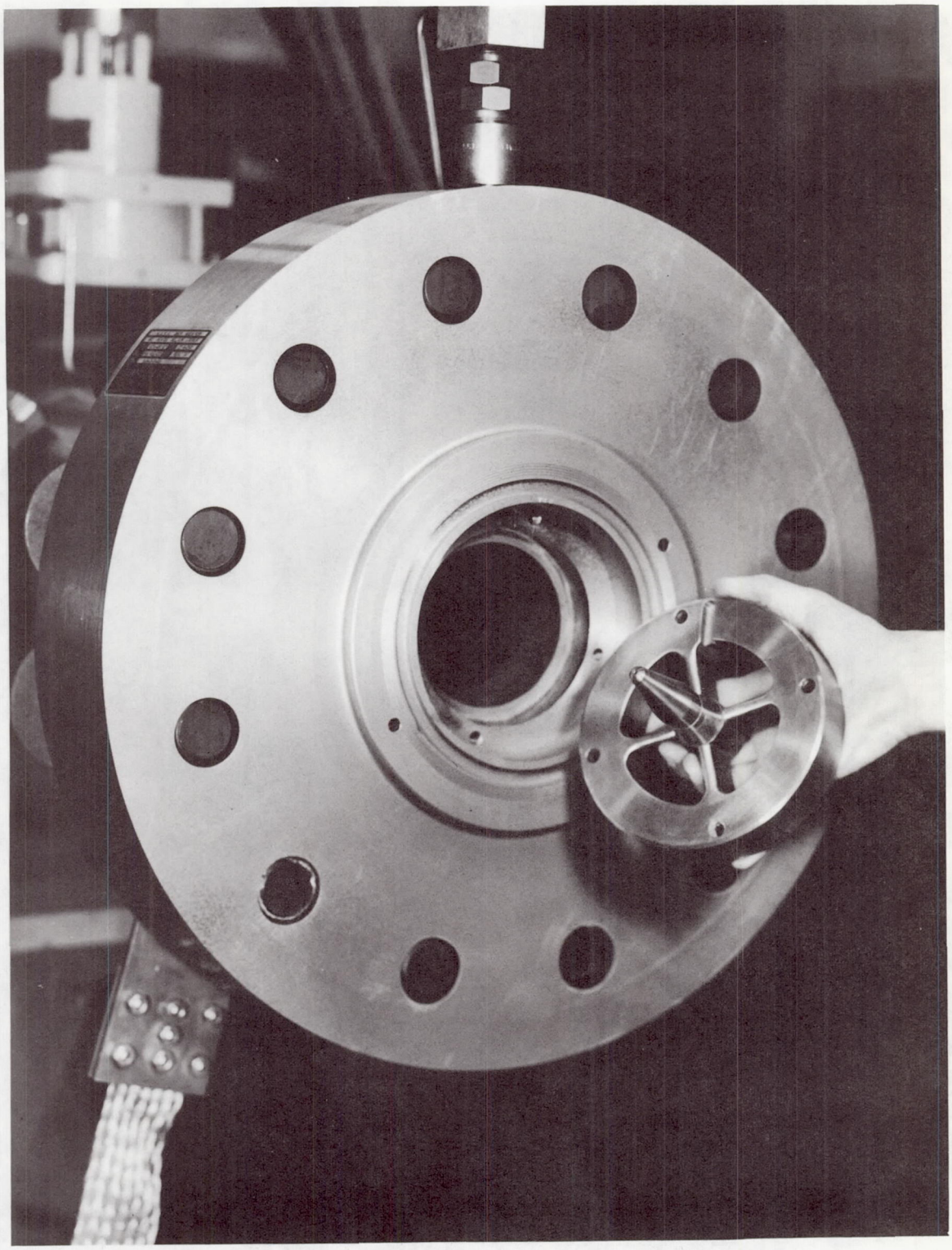

A-36940

Figure 19.- Ground return electrode at downstream end of driver chamber.

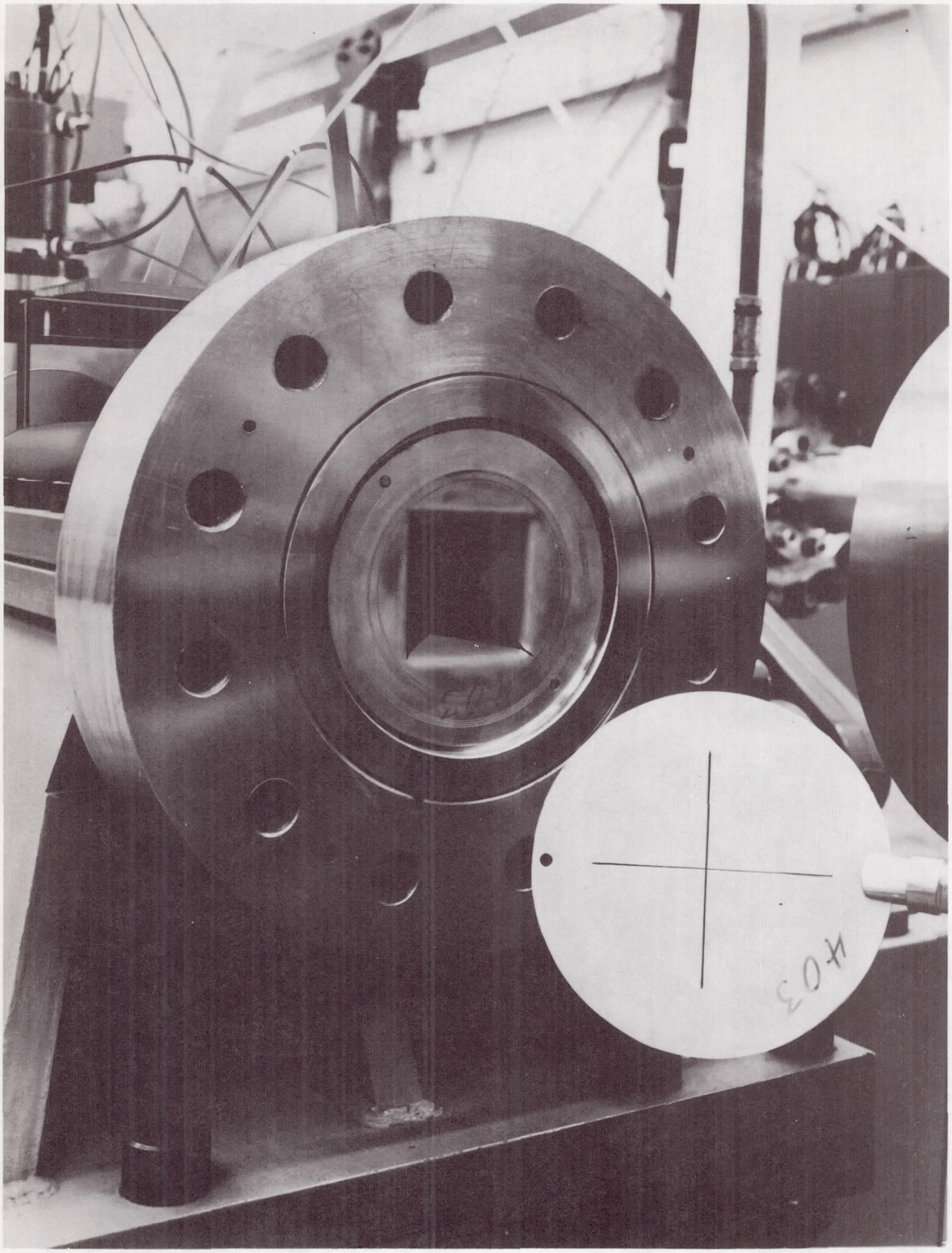

A-41454.1

Figure 20.- Scribing and petaling pattern of diaphragm in holder assembly.

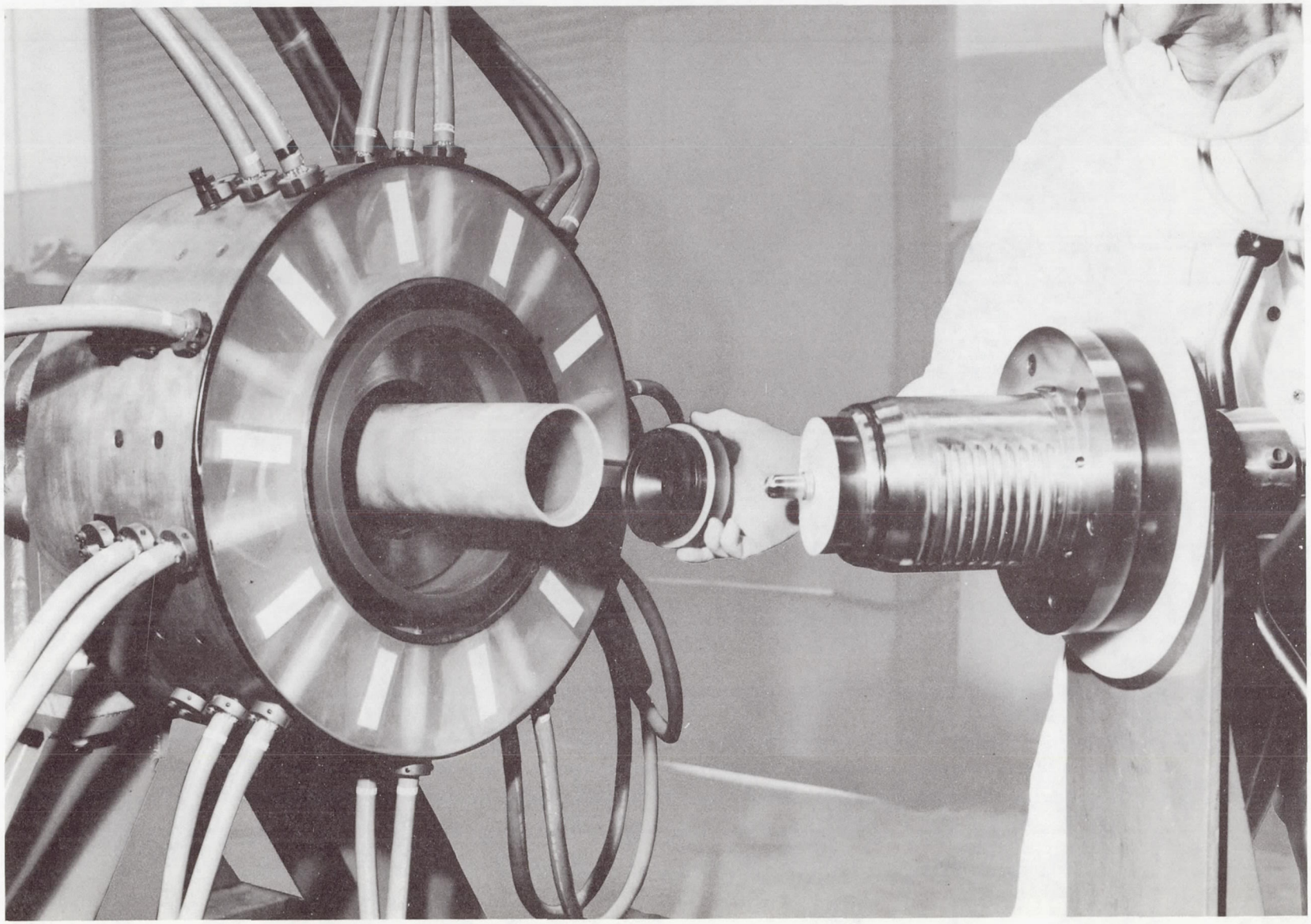

A-41458

Figure 21.- Construction details of liner, breech plug, and high voltage electrode.

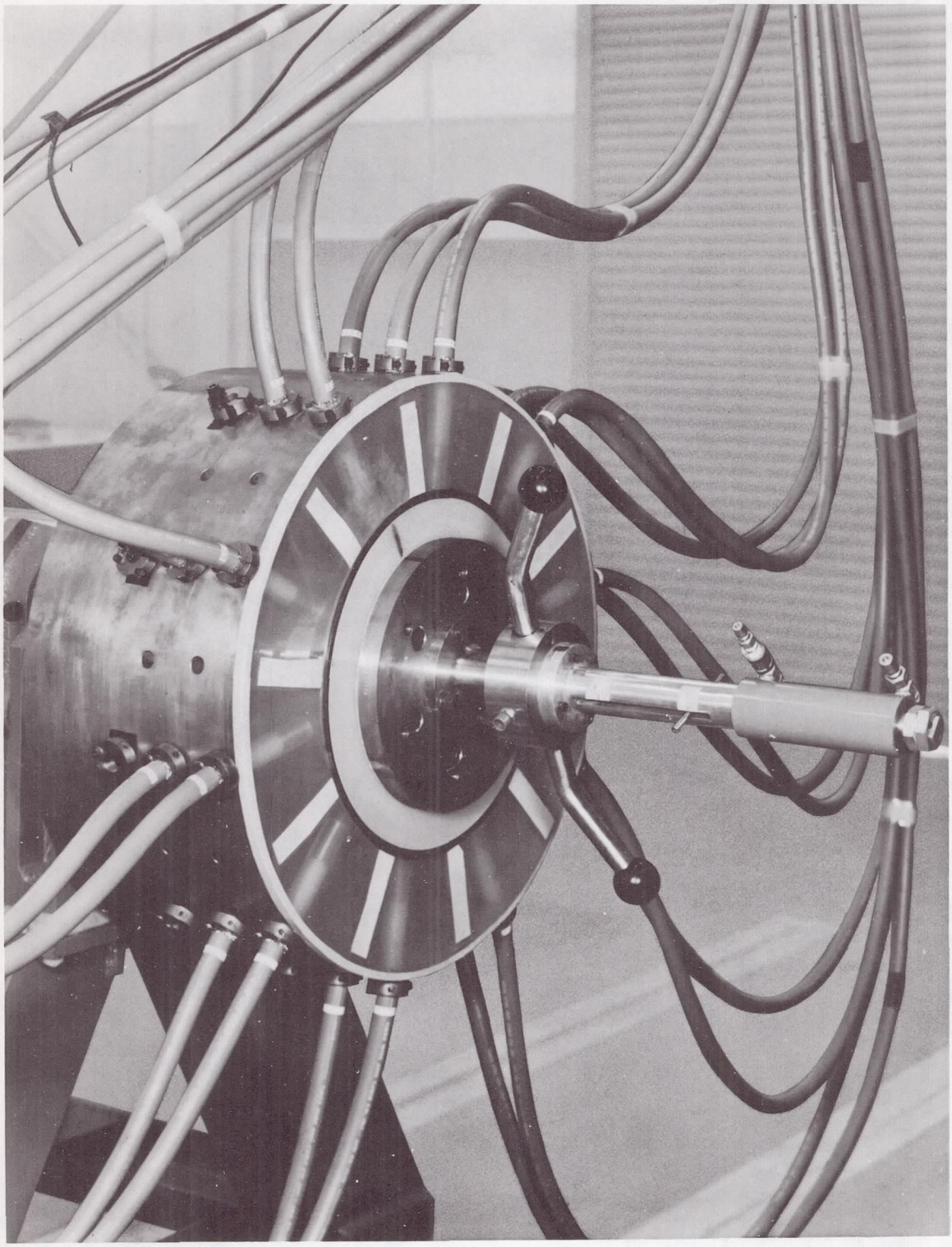

A-36587-1

Figure 22.- Breech installed with electrode assembly isolated from center conductor of cable.

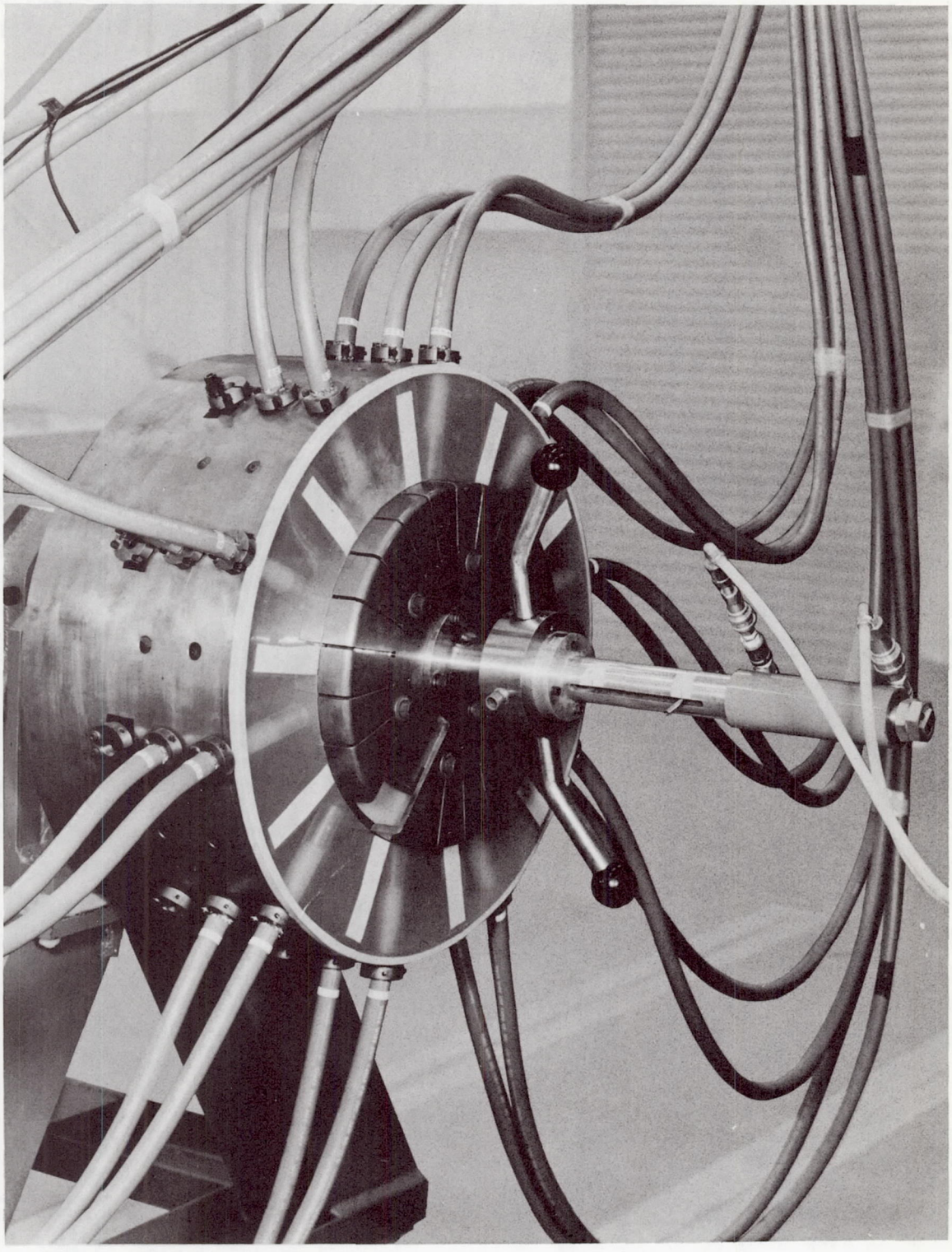

A-36587-2

Figure 23.- Assembled view of breech and contact plate.

NASA-Langley, 1969 —— 11 A-3162